

I hereby declare that I have read through this report entitle “Frequency Response Analysis on Solar Cells and found that it has comply the partial fulfilment for awarding the degree of Bachelor of Electrical Engineering (Industrial Power)

Signature :
اونيورسيتي تيكنيكل مليسيا ملاك

Supervisor's Name : Mohd Shahril Bin Ahmad Khair
UNIVERSITI TEKNIKAL MALAYSIA MELAKA

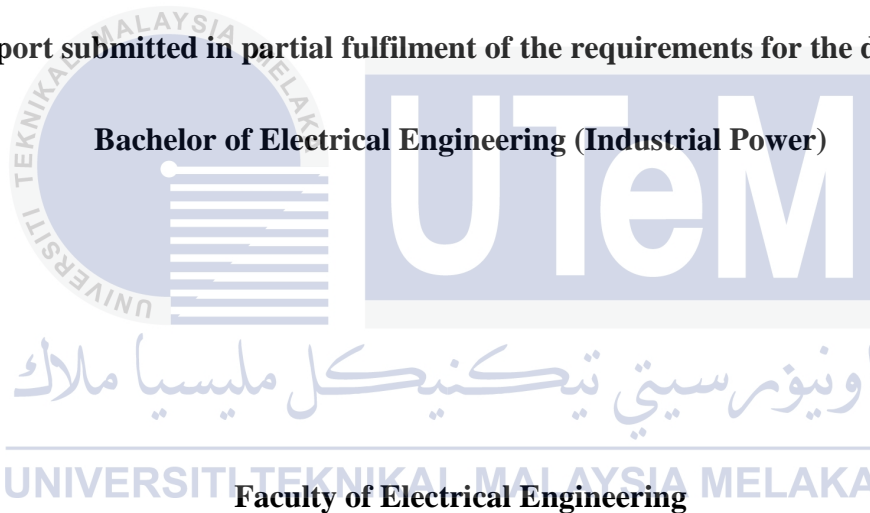
Date : 18/6/2014

FREQUENCY RESPONSE ANALYSIS ON SOLAR CELL

AHMAD UZAIR BIN AHMAD SUHAIMI

A report submitted in partial fulfilment of the requirements for the degree of

Bachelor of Electrical Engineering (Industrial Power)



UNIVERSITI TEKNIKAL MALAYSIA MELAKA

2013

“I declare that this report entitle “Frequency Response Analysis on Solar Cell” is the result of my own research except as cited in the references. The report has not been accepted for any degree and is not concurrently submitted in candidature of any other degree.

اونيورسيتي تيكنيكل مليسيا ملاك

UNIVERSITI TEKNIKAL MALAYSIA MELAKA

Signature :

Name : Ahmad Uzair Bin Ahmad Suhaimi

Date : 18/6/2014

ACKNOWLEDGEMENT

Assalamualaikum warahmatullahi taala wabarakatuh,

First and foremost, I would like to thank to Allah the Almighty for giving me the opportunity to complete my Final Year Project. I would like to thank my supervisor, En Mohd. Shahril Bin Ahmad Khair for his kindness to accept me as one of the students under his supervision. His guidance, encouragement, critics and knowledge have deserved him to receive my biggest appreciation after all this while putting up much effort to see me succeed in completing this project

I would also like to thank my classmates and other Power Engineering lecturers for their support and time in assisting me in completing the project keep and achieve the objectives. Those tips and point of views are valuable enough towards the completion of this project.

Not to forget, my beloved parents, Ahmad Suhaimi bin Zakaria and Sa'adiah Binti Samah for their endless support throughout my studies, for giving me meaningful advices and support me in term of financial support. Being a student handling a project is not easy as people thought. Without parental guidance, support and encouragement, I would not believe that I can have my project completed as it has presented here.

ABSTRACT

Today, from powering a satellite and telescopes in space, to lighting up a solar-powered traffic light on a street; an application of solar energy has rapidly increased and growing over the time. Solar energy is among the renewable energy that important as an alternative to an extinction of fossil fuel generated-electricity like a coal, oil and nuclear energy. It is very significant to comprehend solar cell characteristics in order to study the performance of solar cells. In the real world, manufacturer of solar cell does not include an equivalent circuit model generally or specifically. The circuit is important as it includes the dynamic impedances of solar cells, which are essential in determining the dynamic performance of solar cells. Therefore, with this experiment we can measure and extract the parameter of the circuit using a technique called Frequency Response Analysis (FRA). The main objective for this thesis is to study the function of the FRA device, the Frequency Response Analyzer Bode 100 on a solar cell. Moreover, this thesis will analyze an experimental test for Bode 100 to a solar cell. Then, to study the dynamic impedance of solar cell relationship between different types of solar cells and on different range of DC bias injected to solar cells. The experiment conducted, limit the types of PV modules that tested to two types only, which are 5.5 V 0.85 W poly-crystalline silicon solar cell and 5 V 0.5 W mono-crystalline silicon solar cell. The experiment also uses two amount of different DC bias injected to the solar cell; which are 6 V and 12 V. After design and development of experimental setup takes place, all the data will be capture using software called Bode Analyzer Suite. A frequency injection process runs over the solar cell will produce responses that visualize the pattern of the dynamic impedances. Hence, all the result of the measurement is presented clearly. The result is analyzed through signal processing techniques and comparison techniques. Finally, at the end of this project, dynamic impedances of solar cells have been developed.

ABSTRAK

Hari ini, dari menjanakan satelit dan teleskop di angkasa, hingga menyalakan lampu isyarat solar di jalan; aplikasi tenaga solar telah meningkat dengan pesat dan berkembang dari masa ke masa. Tenaga solar adalah antara tenaga boleh diperbaharui yang penting sebagai alternatif kepada kepupusan bahan api fosil yang menghasilkan elektrik seperti arang batu, minyak dan tenaga nuklear. Adalah sangat penting untuk memahami ciri-ciri sel solar untuk mengkaji prestasi sel solar. Dalam dunia sebenar, pengeluar sel solar tidak menyediakan model litar setara secara am atau secara khusus. Litar ini adalah penting kerana ia termasuk nilai galangan dinamik sel-sel solar, yang penting dalam menentukan prestasi dinamik sel-sel solar. Oleh itu, dengan eksperimen ini kita dapat mengukur dan mengeluarkan parameter litar dengan menggunakan teknik yang dipanggil Analisis Frekuensi Respons (FRA). Objektif utama projek ini adalah untuk mengkaji fungsi alat FRA itu, Frekuensi Response Analyzer Bode 100 pada sel solar. Selain itu, tesis ini akan menganalisis eksperimen untuk Bode 100 dengan sel solar. Kemudian, mengkaji hubungan galangan dinamik sel solar antara jenis sel solar dan pelbagai julat DC bias yang disuntik kepada sel-sel solar. Eksperimen yang dijalankan, menghadkan jenis modul PV yang diuji kepada dua jenis sahaja, iaitu 5.5 V 0.85 W sel solar poli- kristal silikon dan 5 V 0.5 W sel solar mono-kristal silikon. Eksperimen ini turut menggunakan dua jumlah DC berat bias yang berbeza disuntik ke sel solar; 6 V dan 12 V. Selepas reka bentuk dan perkembangan persediaan eksperimen berlaku, semua data akan di tangkap menggunakan perisian yang dipanggil Bode Analyzer Suite. Proses suntikan frekuensi ke dalam sel solar akan menghasilkan tindak balas yang menggambarkan corak galangan dinamik. Oleh itu, semua hasil daripada pengukuran itu dikemukakan dengan jelas. Hasilnya dianalisis melalui teknik pemprosesan signal dan teknik perbandingan. Akhirnya, pada akhir projek ini, galangan dinamik sel-sel solar telah dihasilkan.

TABLE OF CONTENTS

CHAPTER	TITLE	PAGE
	ACKNOWLEDGEMENT	iv
	ABSTRACT	v
	TABLE OF CONTENTS	vii
	LIST OF TABLES	x
	LIST OF FIGURES	xi
	LIST OF ABBREVIATIONS	xiii
	LIST OF APPENDICES	xv
1	INTRODUCTION	1
	1.1 Background	1
	1.2 Motivation	2
	1.3 Problem Statement	2
	1.4 Objectives	3
	1.5 Scope of Study	3
2	LITERATURE REVIEW	4
	2.1 Introduction	4
	2.2 Frequency Response Analysis (FRA) and Earlier Researches	4
	2.3 Principle of Frequency Response	5
	2.4 Principle of Solar Cell	7
	2.4.1 Structure of a Solar Cell	7
	2.5 Crystalline Silicon (c-Si)	9

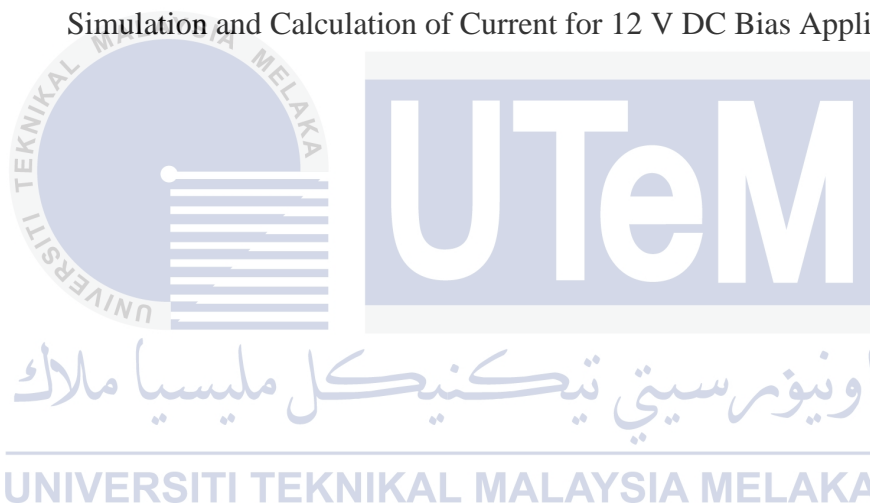
2.5.1 Monocrystalline Silicon Solar Cells	9
2.5.2 Polycrystalline Silicon Solar Cells	10
2.6 Thin-Film Solar Cells (TFSC)	12
2.6.1 Amorphous Silicon (a-Si) Solar Cells	13
2.6.2 Cadmium Telluride (CdTe) Solar Cells	14
2.6.3 Copper Indium Gallium Selenide (CIS/CIGS) Solar Cells	14
2.7 Understanding of Impedance in Solar Cell	15
2.7 Summary of Literature Review	19
3 METHODOLOGY	20
3.1 Introduction	20
3.2 Flow Chart of the Methodology	21
3.3 Detailed Study of Frequency Response Analysis (FRA) and Solar Cells	22
3.4 Design and Development of Experimental Setup	26
3.5 Setup Experiment Test and Data Caption	28
3.5.1 High Impedance Bridge	28
3.5.2 DC Bias Injector	29
3.5.3 Apparatus and Tools Used in Experiment	29
3.5.4 Design Set-Up of the Experiment	31
3.6 Device Configuration, Calibration and Obtaining the Results	32
3.7 Data Analysis	33
3.6 Summary of Methodology	34
4 RESULT AND DISCUSSION	35
4.1 Introduction	35
4.2 Description of FRA Measurements Result	35
4.3 Observation of the Obtained Responses	40
4.4 Discussion of the Obtained Responses	41
4.5 Summary of Results and Discussion	45

5	CONCLUSION	46
	5.1 Conclusion	46
	5.2 Recommendation	47
	REFERENCES	48
	APPENDICES	51



LIST OF TABLES

TABLE	TITLE	PAGE
4.1	Impedance of All DUT at Lowest and Highest Frequency	41
4.2	Extracted Parameter of the DUT Tested	41
4.3	Simulation and Calculation of Current for 12 V DC Bias Applied	43



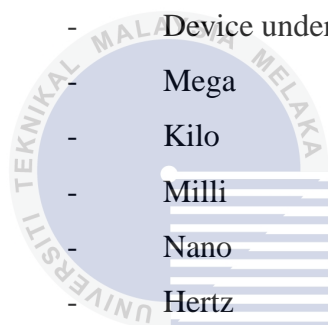
LIST OF FIGURES

FIGURE	TITLE	PAGE
2.1	Linear Transfer Function With Sine Wave Input	6
2.2	(a) Sinewave Input	6
	(b) Steady State Sinewave Response	6
	(c) Corresponding Vector Notation	6
2.3	Typical Solar Cell Structure	8
2.4	A Monocrystalline Silicon Solar Cell Wafer	10
2.5	Polycrystalline Solar Cells	11
2.6	Strong Ribbon Solar Cells	12
2.7	Amorphous Silicon Solar Cell	13
2.8	(a) Cadmium Telluride Solar Cells	14
	(b) Copper Indium Gallium Selenide (CIS/CIGS) Solar Cell	14
2.9	Response of Solar Cell Using 5.6 V DC Bias	17
2.10	Equivalent Circuit Model of the Measured PV module	17
2.11	Real Part of the Various Impedance Responses	18
2.12	Imaginary Part of the Various Impedance Responses	18
3.1	Flowchart of the Project	21
3.2	Interface of Bode 100 Suite Version 2.41 SR1	22
3.3	Measurement Modes Panel	23
3.4	Calibration Toolbar	23
3.5	Frequency Sweep and Configuration Panel	24
3.6	Trace Panel	24
3.7	Plot Space for Graph Visualization	25
3.8	p-Si Solar Cell	26
3.9	mono-Si Solar Cell	26

3.10	12 V GP Battery	26
3.11	4 x 1.5 V GP Battery	26
3.12	Dynamic Equivalent Circuit of Solar Cell	27
3.13	High Impedance Measurement Bridge	28
3.14	Picotest J2130A DC Bias Injector	29
3.15	Apparatus and Tools Used For Measurement and Data Collection Process	30
3.16	Experimental Set-Up of Bode 100 and to Solar Cell (DUT)	31
3.17	Trace 1 and Trace 2 Settings	32
3.18	User Calibration Interfaces	32
4.1	Real and Imaginary Responses of mono-Si, 6 V DC Bias Applied	36
4.2	Real and Imaginary Responses of mono-Si, 12 V DC Bias Applied	36
4.3	Real and Imaginary Responses of p-Si, 6 V DC Bias Applied	37
4.4	Real and Imaginary Responses of p-Si, 12 V DC Bias Applied	37
4.5	Admittance of mono-Si, 6 V DC Bias	38
4.6	Admittance of mono- Si, 12 V DC Bias	38
4.7	Admittance of p- Si, 6 V DC Bias	38
4.8	Admittance of p- Si, 12 V DC Bias	38
4.9	All the Real Responses of the Impedance Obtained from Experimental Procedure	39
4.10	All the Imaginary Responses of the Impedance Obtained from Experimental Procedure	39
4.11	Equivalent Circuit of mono- Si Solar Cell with 12 V DC V Applied	42
4.12	Equivalent Circuit of p-Si Solar Cell with 12 V DC V Applied	42
4.13	of Real Part of Mono-Si vs. Poly-Si on 6 V DC Bias	44
4.14	Responses of Real Part of Mono-Si vs. Poly-Si on 12 V DC Bias	44

LIST OF ABBREVIATIONS

PV	-	Photovoltaic
FRA	-	Frequency Response Analyzer
ECI	-	Electrochemical Interface
DC	-	Direct current
AC	-	Alternating current
DUT	-	Device under test
M	-	Mega
k	-	Kilo
m	-	Milli
n	-	Nano
Hz	-	Hertz
V	-	Volt
W	-	Watt
R	-	Resistor
L	-	Inductor
C	-	Capacitor
S	-	Siemens
F	-	Farad
H	-	Henry
f	-	Frequency
mono-Si	-	Monocrystalline Silicon
p-Si	-	Poly Silicon



اونيورسيتي تيكنيكل مليسيا ملاك
UNIVERSITI TEKNIKAL MALAYSIA MELAKA

LIST OF SYMBOLS

Ω	-	Ohm
μ	-	Micro
ω	-	Angular frequency



LIST OF APPENDICES

APPENDIX	TITLE	PAGE
A	Equivalent Circuit of Mono-Si and P-Si Solar Cell with 6 V DC Bias Applied	49
B	Turnitin Report	50



اونيورسيتي تيكنيكل مليسيا ملاك

UNIVERSITI TEKNIKAL MALAYSIA MELAKA

CHAPTER 1

INTRODUCTION

1.1 Background

Today, from powering a satellite and telescopes in space, to lighting up a solar-powered traffic light on a street; an application of solar energy has rapidly increased and growing over the time. Solar energy is among the renewable energy that important as an alternative to an extinction of fossil fuel generated-electricity like a coal, oil and nuclear energy. Moreover, solar energy is a clean form of energy and this will not give any harm to the environment. Solar energy is generated by a solar panel that is made up of solar cells or known as photovoltaic (PV) cells. It produces electricity by converting the solar light energy to electric energy.

It is very significant to comprehend PV cell characteristics in order to study the performance of PV cells. For application, this includes the basics and expansion of modules, effectiveness assessment and different approaches of measurement. The study of characteristic measurement will resolve information that one may diagnose and developing of material attribute in cell manufacture, to determine PV cell grades for cell manufacture, to validate of appropriate models and to calculate of module operation.

In earlier research of solar cell impedances, it is driven by specialized kit, such as a Frequency Response Analyzer (FRA) using an impedance spectroscopy technique and, an Electrochemical Interface (ECI). In addition, the researches focus on solar cell impedances in term of its elemental properties, and deliberated solar cells under dark surroundings with conditions whether it is forward bias or reverse bias.

1.2 Motivation

Analyzing the solar cell to extract the impedances in it may not be easy to be completed. This project may contribute to an adequate learning of extracting fundamental characteristic and measurement from the solar cell to be analyzed. Frequency response analysis, injected certain range of frequency that reacted with the solar cell to give a response of the characteristic of the solar cell. In previous study of this analysis, there are several methods use to analyze the impedances of the solar cell. There are already recognized familiar methods to analyze the impedance on solar cell, such as Frequency Response Analyzer (FRA) using a technique of impedance and Electrochemical Interface (ECI). FRA using a Vector Network Analyzer – Bode 100 is the new and straightforward way for the condition monitoring technique performs over any devices such as transformer, coaxial cable and eddy-current testing.

1.3 Problem Statement

In the real world, manufacturer of solar cell does not include an equivalent circuit model generally or specifically. The circuit is important as it includes the dynamic impedances of solar cells, which are essential in determining the dynamic performance of solar cells. Therefore, with this experiment we can measure the parameter of the circuit using a technique called Frequency Response Analysis (FRA). FRA is commonly used to test the fault of transformer winding [1]. Today, not only restricted for transformer testing; FRA has widened the application to many other electrical devices. Henceforth, the solar cell will be the next Device Under Test (DUT). The study of this thesis can be implemented in designing efficient, reliable, and ensure the stability of the solar driven power system especially solar cell arrays.

1.4 Objectives

- i. To study the function of the FRA device with Frequency Response Analyzer Bode 100 on a solar cell.
- ii. To analyze an experimental test for FRA Network Analyzer Bode 100 to a solar cell.
- iii. To study the dynamic impedance of solar cell relationship between different types of solar cells and on different range of DC bias injected to solar cells.

1.5 Scope of Study

The scope of this project is to carry out an impedance measurement on different types of solar cells as the DUT. This project uses Bode 100 – The Frequency Response Analyzer unit to extract the dynamic impedance of solar cells under test. Wide-range-and-various-level of frequency of 10 Hz to 100 kHz is injected into the PV module to impedance measurement data that will be analyzed through signal processing techniques – comparison and signature technique. The measurement that will be done is in “impedance vs. frequency” and this kind of measurement will be done throughout the procedure. The measured impedance will be in real and imaginary. These experiment will limit the PV modules that will be test by only two type which are 5.5 V 0.85 W poly-crystalline silicon solar cell and 5 V 0.5 W mono-crystalline silicon solar cell. Furthermore, two amount of different DC bias will be injected to the solar cell; which is 6 V and 12 V. Process of study the PV modules characteristic, identify the types of PV module and analyze the PV modules under test will be performed through this project step by step in order to obtain desired objectives.

CHAPTER 2

LITERATURE REVIEW

2.1 Introduction

This chapter explains the related information in order to increase the significance of studying the project. Frequency Response Analysis (FRA) is studied based on its history of earlier use of the technique. Subsequently, this chapter explain about the principle of frequency response and principles of solar cell. Then, types of solar cell, crystalline silicon solar cells and thin-film solar cells is studied and explained clearly. Lastly, this chapter explain about the understanding of impedance in solar cell.

UNIVERSITI TEKNIKAL MALAYSIA MELAKA

2.2 Frequency Response Analysis (FRA) and Earlier Researches

FRA is an essential test implement for the measurement of some dynamic systems. Dynamic system is caused by the impedance of the material being tested that is DUT. Impedance generally consists of a resistor (R), inductor (L), and a capacitor (C). The test is established by injecting input of oscillated frequency to a steady process and gives an output of oscillated frequency but mismatched in term of amplitude and phase. Typically use in a power transformer, FRA is specifically used to determine the impedance of the winding over a broad spectrum of frequencies as seen in [1]. The outcome is then set side by side of the reference data set and the variance shall be making used to figure out the category and fault region. Vital broad spectrum of frequencies is injected by either two

steps, through inserting a pulse into the transformer winding or by applying a sinusoidal wave to do a frequency sweep. The previous technique is called impulse response method and recently known as the swept frequency method. A graph of the amplitude against frequency is plotted from the result and it is used for comparison for the two sets of measurement. Vital changes like a modulation to the pattern of the curve, the development of new resonant frequencies or the withdrawal of current resonant frequencies and huge deviation of current resonant frequencies. FRA is a convinced and competent medium of finding a deficiency in transformer. The major importance of the method belongs in its capability to find faults but nowadays researchers have found various usage of FRA in other DUT. Among of it are solar cell impedance measurement, small signal transformer analysis, battery impedance measurement, equivalent circuit analysis of quartz crystals and low value impedance measurements. Instead of finding fault in DUT, frequency response analysis is used to find the impedance in solar cell for other means. Impedance in a solar cell is a critical specification to observe as it is symbolic to the aging and consequences of sustaining life period of the solar cell. As stated in [2], variations in this parameter deriving out of guideline shall be applied to evaluate the aging period or fault in the solar cell. Moreover, the study can use to create an adequate, decent, eminent power and small-scale switching power conditioner.

2.3 Principle of Frequency Response

Frequency response is widely recognized to define a specific system in the concept of its dynamic. Meanwhile, frequency response analysis is the method whereby a sine wave is injected to a DUT to measure notches on the frequency response of a transfer function or impedance function [3]. The output – in contrast with the input – as a function of frequency commonly in magnitude and phase measurement. As a matter of fact, frequency response is a fluctuation of the gain and phase with distinct frequency. The fundamental arrangement is presented in Figure 2.1 in which a sine wave $u(t)$ is implemented to a system with transfer function $G(s)$.

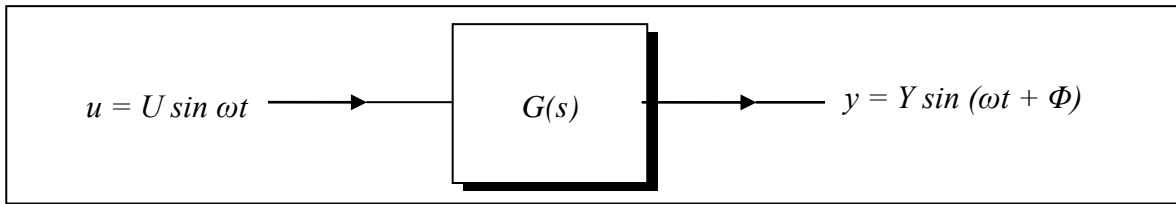


Figure 2.1: Linear Transfer Function with Sine Wave Input [3]

After transients due to earliest circumstances have disintegrated away, the output $y(t)$ turn into a sine wave but with a different magnitude Y and relative phase Φ . The output $y(t)$ are factually related to the transfer function $G(s)$ by magnitude and phase, at the frequency (ω rad/s) of the input sinusoid.

$$\frac{Y}{U} = |G(j\omega)| = \text{gain at } \omega \quad (2.1)$$

And
$$\Phi = \angle G(j\omega) = \text{phase at } \omega \quad (2.2)$$

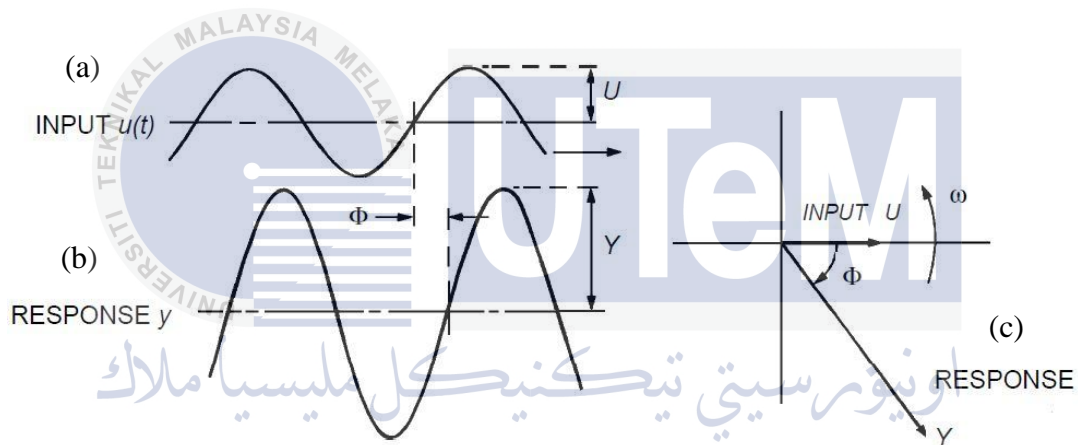


Figure 2.2: (a) Sinewave Input. (B) Steady State Sinewave Response. (C) Corresponding Vector Notation [3]

By nature of the electrical device, in theory they have some resistance, inductance and some capacitance values. Accordingly, the complex RLC circuit is formed without exception in every of them. The label 'theoretical' imply several devices should have very little or no resistance correlated to their inductance and capacitance values over, several devices should have very little or no inductance correlated to their resistance and capacitance and over several devices should have very little or no capacitance correlated to their resistance and inductance but theoretically all of them can be analyzed as an RLC circuit notwithstanding may be $R = 0$, or $L = 0$ or $C = 0$. However, in nearly all cases the resistance, inductance and capacitance of equipment have values (non-zero).

Consequently, the majority of the electrical equipments can be viewed as an RLC circuit thus they give feedback to the frequencies injected and produce a unique indication.

2.4 Principles of Solar Cell

Solar or photovoltaic (PV) cells are comprised of materials that convert sunlight into electricity. PV technologies along with Concentrating Solar Thermal Plant (CSP) are sustainable energy technologies and are clean energy alternatives, as we are aware, most of the energy consumed today is non-renewable. Moreover, the energy is unclean such as the burning of the fossil fuels. PV cells consist of coatings of semiconductors for example, silicon. Energy is generated when photons of light from the sun collides a solar cell and are captivated inside the semiconductor material. This energizes the semiconductor's electrons, result in the electrons to discharge, and produce an electric current [4]. The electricity created is direct current (DC) since the flows of charge is in one direction. One PV cell generates only one or two watts which is not a practical power for most usages. In order to boost power, PV cells are arranged together into what is called a module and packaged into a form which is more usually known as a solar panel. Solar panels that grouped are later called solar arrays [5].

2.4.1 Structure of a Solar Cell

A typical solar cell is a multi-coated unit composed of:

- i. Cover glass. A transparent glass or plastic layer that supports exterior safety from the elements.
- ii. Anti-reflective Coating. This element is invented to avoid the light that reaches the cell from rebound so that the peak energy is absorbed into the cell.
- iii. Front Contact. Conducts the electric current.
- iv. N-Type Semiconductor Layer. A thin layer of silicon, mixed with phosphorous using a method called doping to produce a better conductor.
- v. P-Type Semiconductor Layer. A thin layer of silicon mixed or doped with boron to produce a better conductor.
- vi. Back Contact. Conducts the electric current.

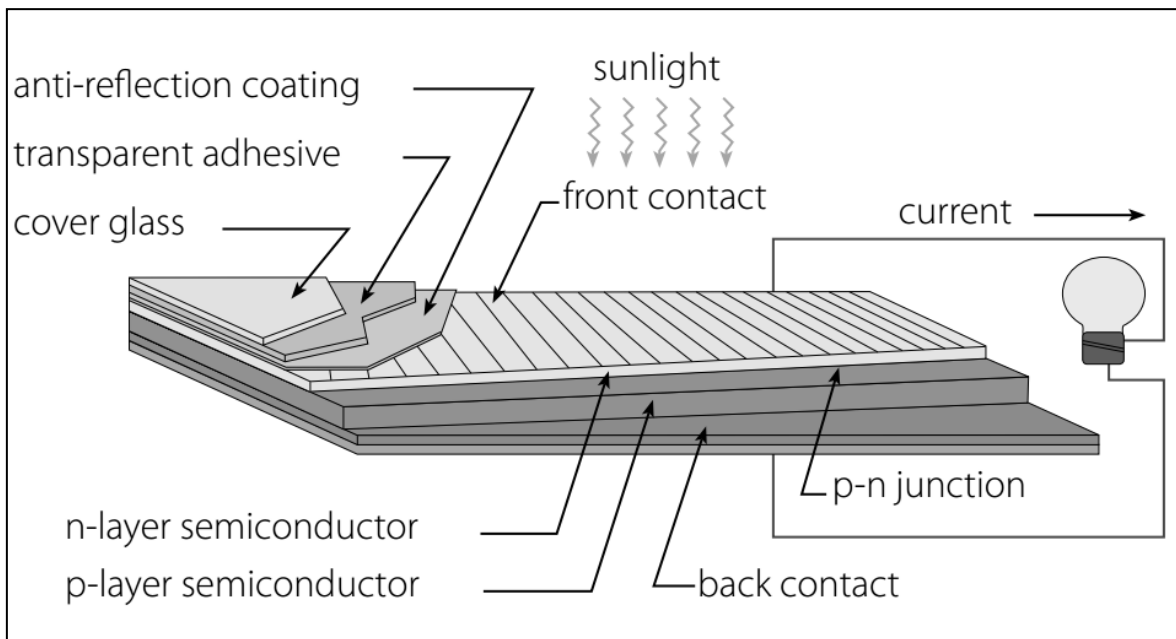


Figure 2.3: Typical Solar Cell Structure [5]

After the layers have been assembled, there is a negative charge in the p-layer and a positive charge in the n-layer region of the junction [4]. This causes lack of balance in the charge of the two layers at the p-n junction. Thus, creates an electric field in the middle of the p-layer and the n-layer. If the PV cell is located in the sun, radiating energy of the sun hits the electrons in the p-n junction and triggers them, hitting them loose of their atoms. These electrons are attracted to the positive charge in the n-layer and are repelled by the negative charge in the p-layer. A wire can be connected from the p-layer to the n-layer to form a circuit. The free electrons are accelerated into the n-layer of the radiant energy, resulting to beat off each other. The wire conducts a path for the electrons to flow away from each other. Current is caused by the movement of electrons and voltage is caused by the electric field of the cell. Hence, power is produced, by the product of current and voltage [4].

2.5 Crystalline Silicon (c-Si)

Nearly 90% of the PV modules manufacturers around the world now are established on some variation of silicon [4]. As mentioned in [4], about 95% of all consignments of U.S. producers in the residential zone were c-Si panels in 2011. The fundamental characteristic is the purity of the silicon [5]. Silicon purity is when the silicon molecules are coordinated to perfection. The perfect the arrangement, the prominent the cell intend to be at converting solar energy (from the sunlight) into electricity (the photoelectric effect). The efficiency of PV cells is associated with purity. Besides efficiency, cost and space-efficiency are reason in choosing the PV cells. Crystalline silicon forms the basis of mono- and polycrystalline silicon solar cells:

2.5.1 Monocrystalline Silicon Solar Cells

Monocrystalline silicon (mono-Si), also known as single-crystalline silicon (single-crystal-Si), are commonly known by an even surface coloring and systematic appearance, shows that it is high-purity silicon as shown in Figure 2.4 [5]. Mono-Si solar cells are made out of silicon mold that is cylindrical in configuration. Four edges of the cylinder-shaped molds are removed out to form silicon substrate, to maximize performance and reduced costs of an individual mono-Si cell, resulting in mono-Si panels their characteristic presence. A good way to separate mono- and polycrystalline solar panels is that polycrystalline solar cells look perfectly rectangular with no rounded edges. The advantages of mono-Si panel are it has the highest efficiency percentages, space-efficient, long life and tend to perform better than similarly rated polycrystalline PV panels at low-light conditions. Mono-Si panel are invented among the topmost quality silicon, hence they have the highest efficiency percentages. It is space-efficient since these PV panels produce the highest power outputs; they also need the smallest amount of space distinguished to any other types. Furthermore, it generates up to four times the amount of electricity as thin-film PV panels. Mono-Si panels also have the longest lifespan. Nearly all PV panel manufacturers put a 25-year warranty on their mono-Si panels. The disadvantages of mono-Si panels are it is the most costly. In addition, if the panel is fractionally closed with shadow, dirt or snow, the whole circuit can malfunction. Besides, the Czochralski process is used to manufacture monocrystalline silicon which results in large cylindrical mold.

Four sides are removed out of the molds and, leave a serious amount of the original silicon, ends up as misuse.



Figure 2.4: A Monocrystalline Silicon Solar Cell Wafer [5]

2.5.2 Polycrystalline Silicon Solar Cells

Introduced to the market in 1981, also is known as polysilicon (p-Si) and multi-crystalline silicon (mc-Si). P-Si panels do not involve the Czochralski process, contradictory to mono-Si panels. Raw silicon is melted and let flow into a square mold, which is cooled and trims into totally square wafers. There are several advantages of p-Si. The method used to prepare them is simple and inexpensive. Moreover, it does not waste a lot of silicon as to mono-Si. Others, p-Si cell likely to accept marginally lower heat tolerance than mono-Si. High temperature can influence the performance of solar panels and reduce their lifespan. On the contrary, p-Si cells are not as efficient as mono-Si cells might be. The efficiency is usually 13-16% because of less silicon purity [5]. Furthermore, this type has a lower space - efficiency. In order to get the same power output as the mono-Si, normally it covers a larger surface.

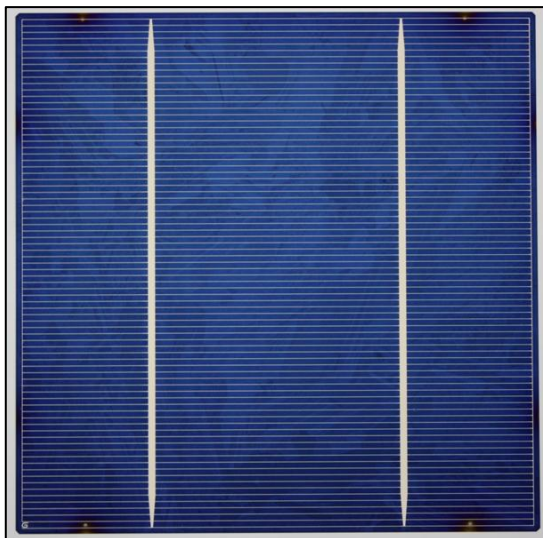


Figure 2.5: Polycrystalline Solar Cells [5]

2.5.2.1 String Ribbon Solar Cells

String Ribbon PV panels are another type of polycrystalline silicon based PV panel. String Ribbon is actually the name of a manufacturing technology that fabricates a pattern of p-Si. It is made by pulling temperature-resistant wires throughout melted silicon, which develops a very thin silicon ribbons. String Ribbon PV panels look identical to conventional polycrystalline PV panels. The advantages of String Ribbon PV panels are it only uses half the amount silicon as mono-Si manufacturing. This contributes to lower costs. Moreover, String Ribbon PV panels have the lowest space-efficiency of any of the main types of crystalline-based solar panels. Apart from that, String Ribbon PV panels are somewhat more energy extensive and more expensive. Efficiency is at best on par with the low-end polycrystalline solar panels at around 13-14% [5]. In research laboratories, researchers have pushed the efficiency of String Ribbon solar cells as high as 17.8% [6].

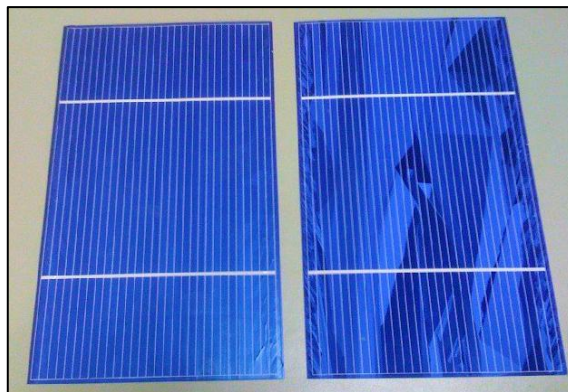


Figure 2.6: Strong Ribbon Solar Cells [5]

2.6 Thin-Film Solar Cells (TFSC)

By transferring one or a few thin coats of photovoltaic material onto a wafer, thin-film solar cells are manufactured. It is also called as thin-film photovoltaic cells (TFPV). The various types of TSFC can be classified by which PV element is deposited onto the substrate [7]:

- Amorphous silicon (a-Si)
- Cadmium telluride (CdTe)
- Copper indium gallium selenide (CIS/CIGS)
- Organic photovoltaic cells (OPC)

Relying upon the technology, early pattern of thin-film module have shown efficiencies in the range of 7–13% and about 9% for manufactured modules. Imminent module efficiencies are predicted to reach about 10–16% [8]. The benefits of this type are mass-production is simple and cheap, it can be built flexible, heat and shading has a minor consequence of TFSC performance. Although, there is a downside of TFSC since generally it is not very useful for most residential situations. Besides cheap, they require a lot of space. TFSC tend to degrade faster than mono-Si and p-Si solar panels.

2.6.1 Amorphous Silicon (a-Si) Solar Cells

Suitable for small-scale applications, amorphous silicon (a-Si) based PV cells have low power output. Yet, current modifications have invented them more interesting for a few big-scale applications too. Several coats of a-Si solar cells can be combined using a method called “stacking”, which produces in greater efficiency rates (normally around 6-8%) [7]. Only 1% of the silicon used in crystalline silicon solar cells is required in amorphous silicon solar cells. On the contrary, stacking is costly.

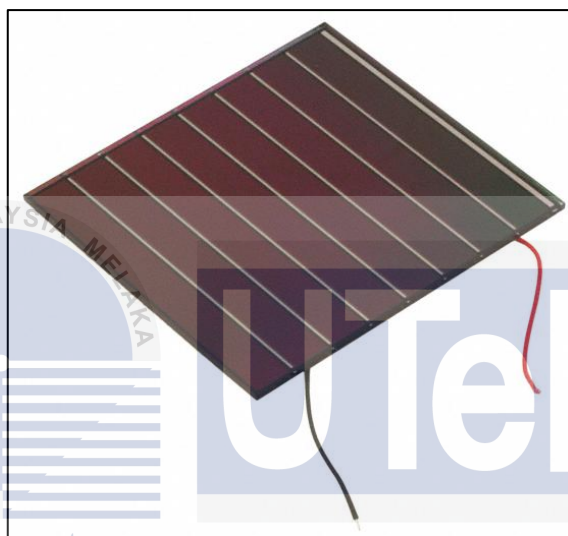


Figure 2.7: Amorphous Silicon Solar Cell [7]

2.6.2 Cadmium Telluride (CdTe) Solar Cells

Cadmium Telluride Figure 2.8 (a) is the only TFSC that has exceeded the cost-efficiency of crystalline silicon solar panels in a compelling fraction of the market (multi-kilowatt systems). The efficiency of CdTe cells usually operates in the range of 9-11%. First Solar CdTe solar module reached the efficiency of 14.4% as in [9].

2.6.3 Copper Indium Gallium Selenide (CIS/CIGS) Solar Cells

CIGS solar cells (Figure 2.8 (b)) have showed the most potential in terms of efficiency compared to the other TFSC above. These PV cells contain lower numbers of the toxic material cadmium that is found in CdTe solar cells. The efficiency rates for CIGS solar panels typically operate in the range 10-12 % [7]. Many TFSC types are still early in the research and testing stages. Some of them have enormous potential.

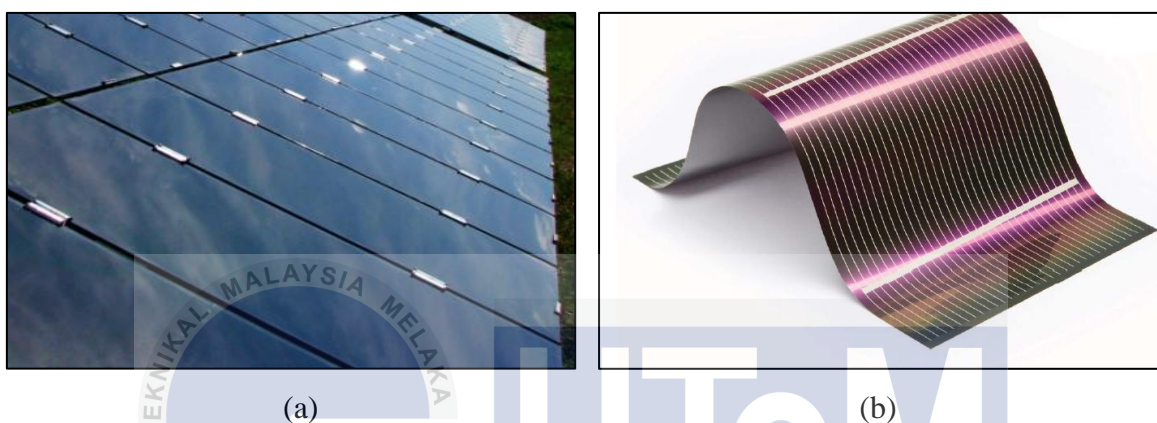


Figure 2.8: (a) Cadmium Telluride Solar Cells. (B) Copper Indium Gallium Selenide (CIS/CIGS) Solar Cell [9]

2.7 Understanding of Impedance in Solar Cell

When building or designing the solar power system, impedance in a solar cell is among the factor taken. In a PV system, it is very important to optimize the size of each component in order to increase efficiency of the technical and economic factor. To find out, the study the fundamental of the theory of “electrical impedance” is important.

As mentioned in 2.4, PV system arrays will produce DC. The current then flows through an inverter and convert it to AC, which then to be fed to electricity grid or directly used to power appliances. Electrical impedance is the frequency domain ratio of voltage to current, mainly a resistance but for AC current. In other words, current in the AC circuit flow between two positions is constrained by impedance.

In a PV system, while the earliest set of electrons flows through the wires it is in a DC form that connect the PV panel to the inverter, to convert the current form to AC to match the electrical grid current form; despite there are some constraint here [10]. The transmission of electricity around a network is generally divided into three forms which are large, medium and small distribution and transmission. The logic for the three different sizes is to decrease the losses which happen during the delivery of electricity over long distances. Moreover, the different sizes are based on the estimation of the amount of energy will be consumed by the area. Some power lines are sized to 330kVA while, some are designed to 110kVA or even less. The size of these power lines is predetermined by electric companies such as Tenaga Nasional Berhad (TNB) and Sabah Electricity Sdn Bhd and if you build a PV system and its output does not match the voltage and phase of the power line that connects to, there will be an impedance mismatch will result in losses.

Impedance matching is a significant concept because impedance acts as resistance to the power that is delivered back to the network. In essence, the actual amount of power received by the network is reduced and thus reduces the efficiency of your solar energy system [10]. A large solar power system cannot feed into a point towards the end of the grid without certain adjustments to your system, in this case an inverter. Therefore, when considering the size of your inverter, it is important to determine not only the most appropriate size of the system based on your requirements, but also the best size based on what the network is able to accept from you at the connecting point of your meter.

For modelling of a solar cell or a PV module, a DC model or DC equivalent circuit is adequate for describing solar array behaviour in general. A DC circuit model consists of a series resistance (R_s), a shunt resistance (R_{sh}) and a diode having a non-ideal diode factor [10]. The solar cells dynamic characteristics and impedance measurements had been described and reported in some specific applications, such as satellite applications [11, 12], the Mars Pathfinder and measurement of impedance of GaAs/Gc solar cells [13] and the Si Back Surface Field Reflector (Si-BSFR) solar cells [13]. The results are used to design efficient, reliable, high power devices with stability. In all cases, the impedances are determined by special equipment, such as an ECI, FRA using an impedance spectroscopy technique. In previous studies, they highlight solar cell impedances in terms of material properties, and measured solar cells under dark conditions with either forward bias or reverse bias conditions. The understanding of dynamic impedances of solar cells and arrays is essential in determining the dynamic performance of arrays when connected to

electricity distribution networks. It will become increasingly important when more PV systems are connected to the networks.

Figure 2.8 below is an experiment conducted in [14]. The experiment used a 5.6 V of DC bias which is 8 cells of 0.7 V per cell connected in series. As the result from the response, the equivalent circuit model of the measured PV module is produced (Figure 2.9). On the contrary, this model is only valid for 5.6 V DC bias and the parameter is controlled by the amount of DC voltage injected to the PV cell as much as the amount of the light exposed to the cell.

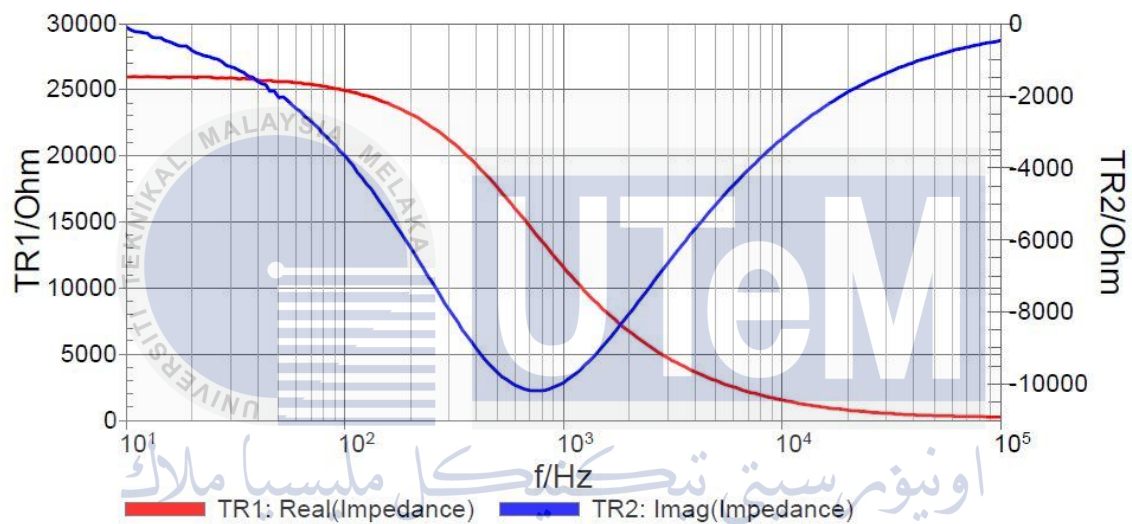


Figure 2.9: Response of Solar Cell Using 5.6 V DC Bias [14]

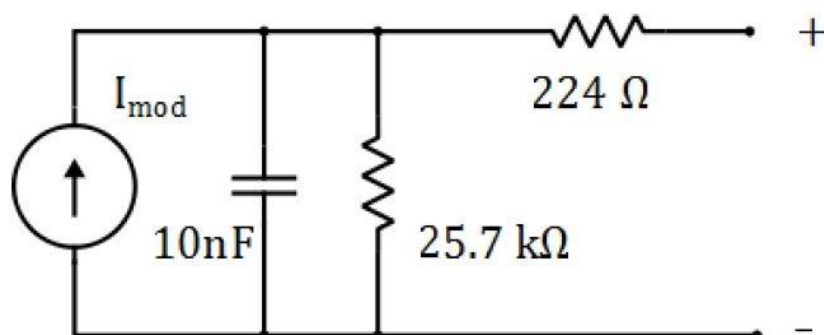


Figure 2.10: Equivalent Circuit Model of the Measured PV module [14]

Respectively, the DC bias influenced the parameter of the response. Which resulting in different results for different voltage injected. The following responses, Figure 2.10 and 2.11 shows the real and imaginary part of the PV cell impedance, variously from 0.55 V, 0.6 V, 0.65 V and 0.7 V per cell (8 cells are arranged in series) [14].

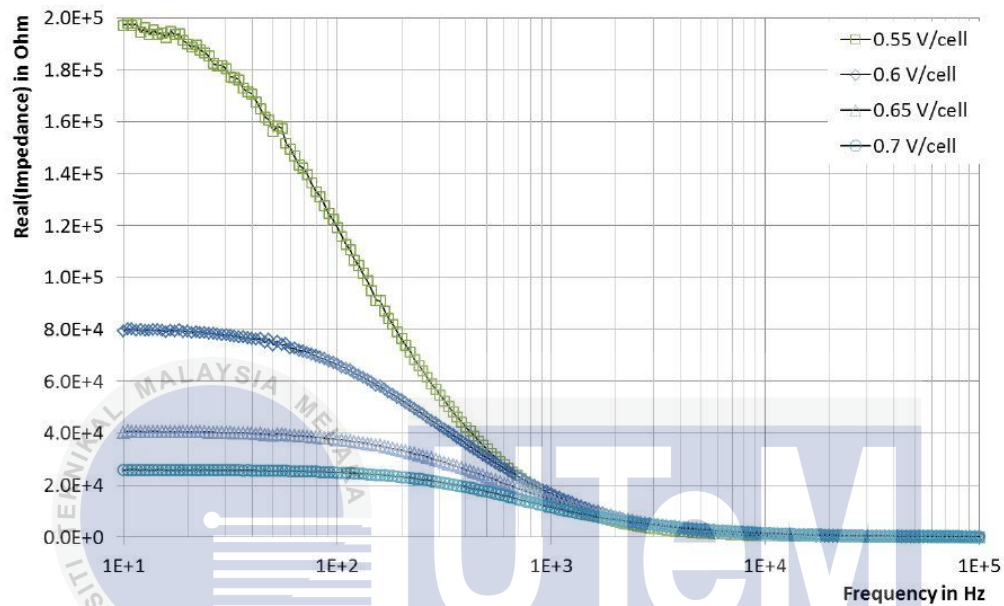


Figure 2.11: Real Part of the Various Impedance Responses [14]

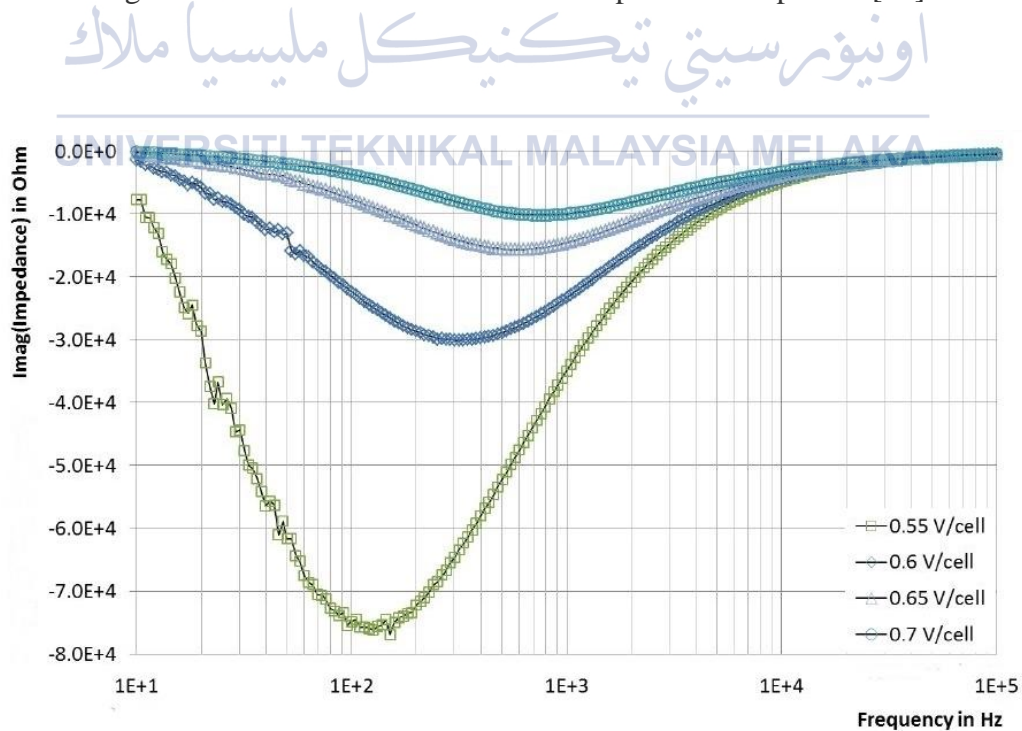


Figure 2.12: Imaginary Part of the Various Impedance Responses [14]

2.8 Summary of Literature Review

In this chapter, all the related information for the project completion is stated. The Frequency Response Analysis (FRA) is discussed and as the main motivation for this project, an explanation of how it works is explained further. In addition, frequency response and typical resistor (R), inductor (L) and capacitor (C) responses are discussed. Frequency response discusses about how to obtain transfer function and response besides the study of the previous researches. Principles of solar cells are explained thoroughly throughout the chapter together with the various types of solar cell. For better understanding of the project objectives, fundamental of the impedance of solar cell is studied and explained.

CHAPTER 3

METHODOLOGY

3.1 Introduction

In this chapter, it is stated the process of the project from the beginning to the very detail procedure of obtaining the result and is finished with data analysis. The flowchart in Figure 3.1 describes the continuous process with the representation of phase by phase. The next section, it gives a clearer view on every phase completion starting with literature review and preliminary study, design and development stage, testing and measurement, data caption and end with data analysis. Every phase is explained in detail to ease the project completion.

3.2 Flow Chart of the Methodology

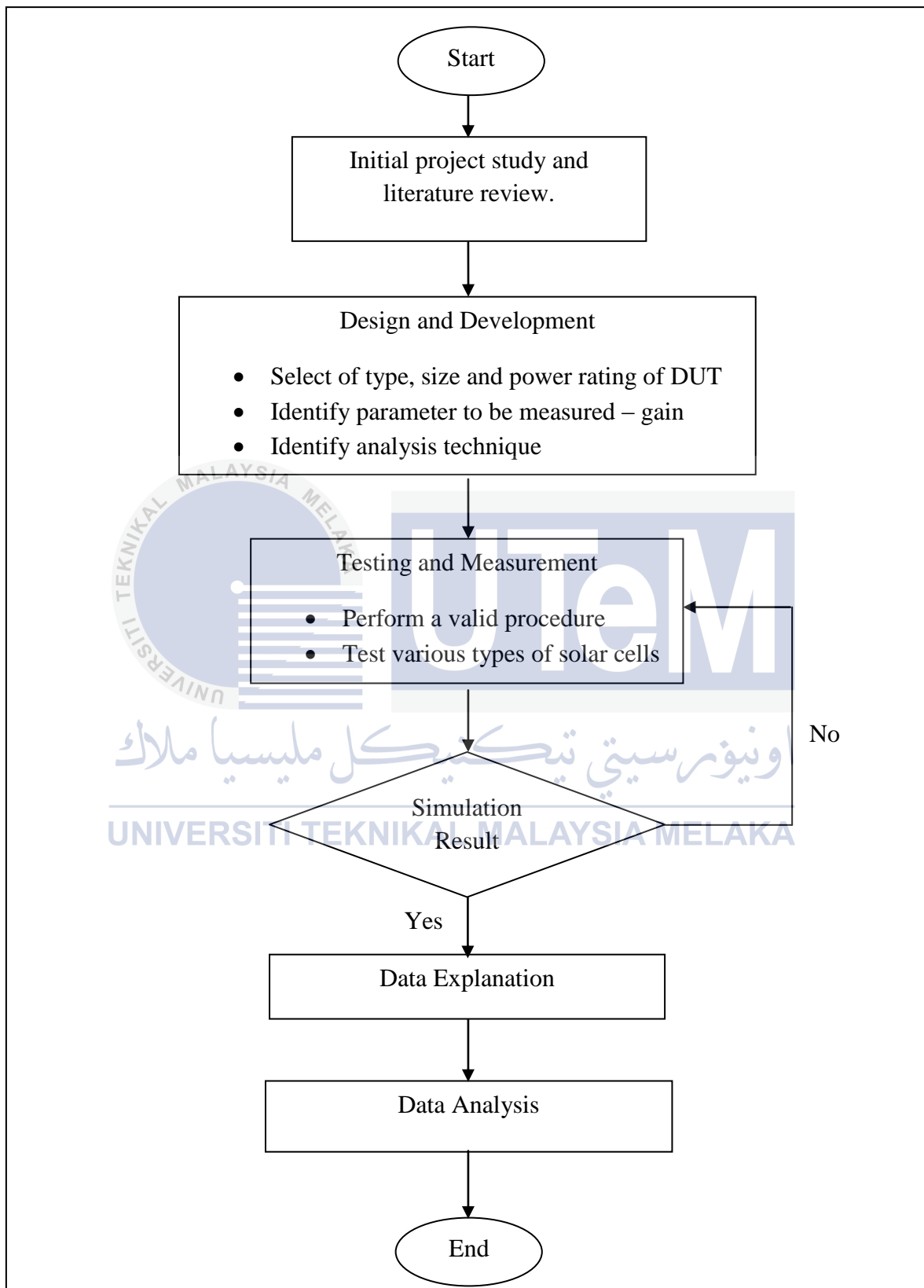


Figure 3.1: Flow Chat of the Project

3.3 Detailed Study of Frequency Response Analysis (FRA) and Solar Cells

This part is all about mentioning the preliminary studies should be done before proceeding to the second phase. Firstly, is to get to know the main item for this project, the network analyzer. The network analyzer or FRA device called Bode 100 can do many important measurements that performed on the specified DUT. The DUT is typically a transformer; however, this project aims to implement the use of Bode 100 to analyze solar cell impedance. Bode 100 is capable of handling measurements as gain or phase, impedance and frequency sweep. Figure 3.2 shows an overview of the suite of Bode 100.

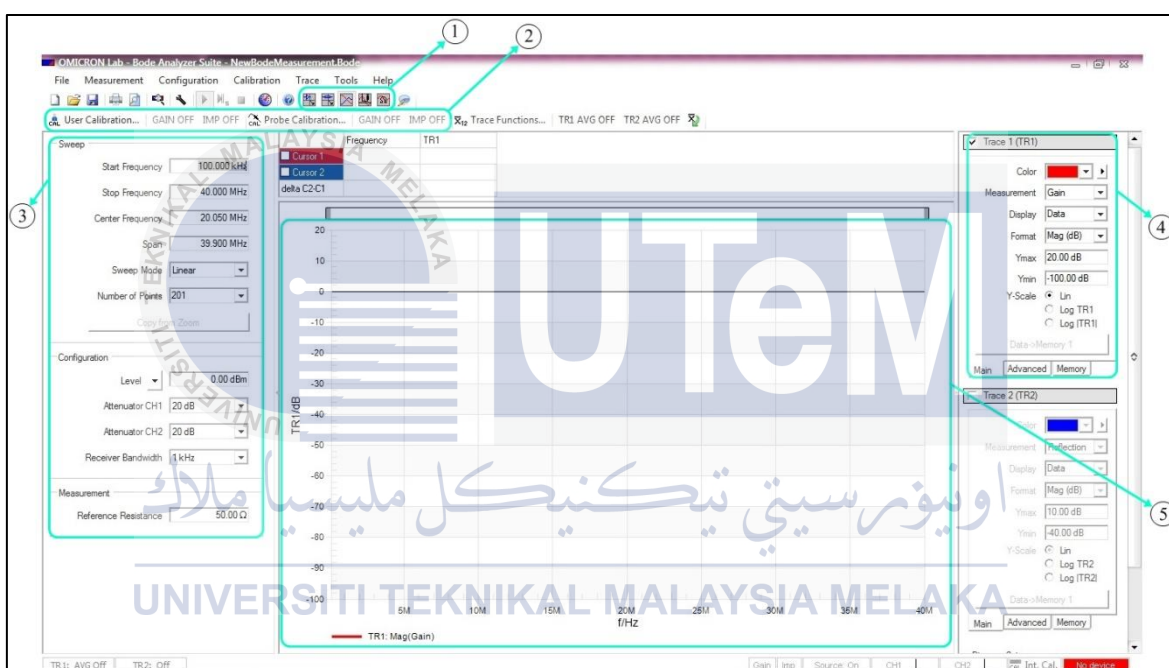


Figure 3.2: Interface of Bode 100 Suite Version 2.41 SR1

Figure 3.3 shows five measurement modes available that can be performed by Bode 100. It consists of the gain/phase, impedance/reflection, frequency sweep, frequency sweep (external coupler) and frequency sweep (impedance adapter). These modes may be useful, and either of the two modes can be used for verification of a result. For example, mode impedance/reflection can be used to measure impedance of special DUT. For fair comparison, frequency sweep mode can also be used to measure impedance of a DUT. The result is the same however; the technique could be slightly different.

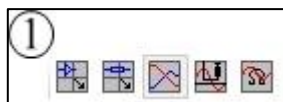


Figure 3.3: Measurement Modes Panel

Figure 3.4 is the calibration toolbar. The Bode 100 can offset the effects of the measurement setup like cables and probes. In addition to the overall accuracy may be improved by calibrating the Bode 100. The Bode 100 supports two methods of calibrating: the Probe Calibration optimized for measurements that require frequent changes of measurement configuration and User calibration for more accurate results.



Figure 3.4: Calibration Toolbar

Figure 3.5 represents a column on the left side of the software. It consists of the start and stop frequency that user aim to use. However, the value of the maximum frequency can be set is 40MHz. Sweep, The upper box indicating amount of frequency that is injected into the device under test from the specification initially set in the start and stop frequency column provided. The middle box is settings that control the smoothness of the graph produced. The attenuator shows the attenuation level of demand can be used in graph prepared with the starting range from 0 dB to 40 dB. The bottom panel is part showing measurement reference resistance is 50Ω. This resistance will be use throughout the session.

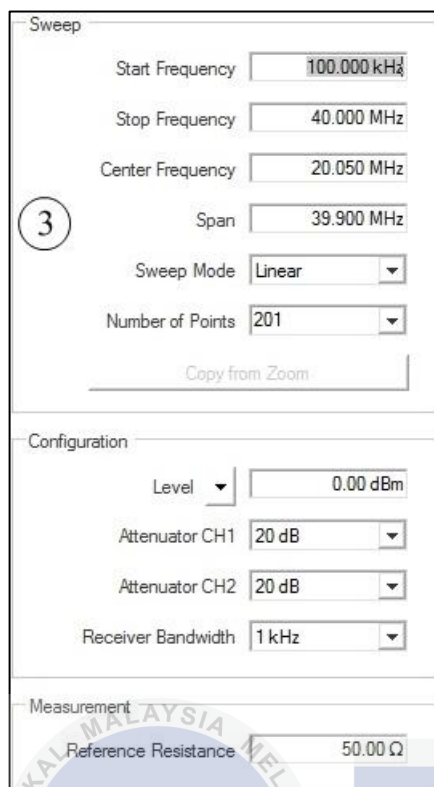


Figure 3.5: Frequency Sweep and Configuration Panel

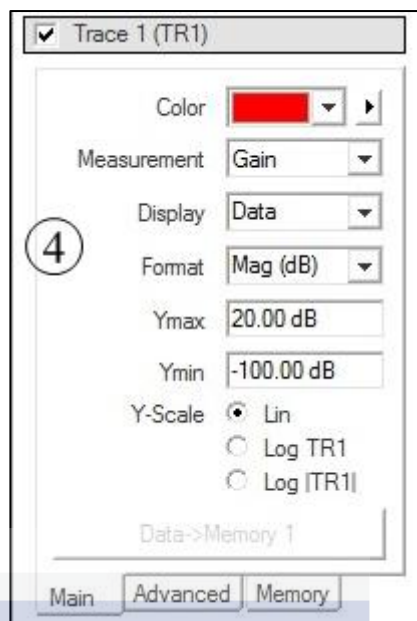


Figure 3.6: Trace Panel

Figure 3.6 shows trace panel. It has two traces which indicate two measurements. It can be plot in the same space or separately and each trace has the same function and can be used simultaneously with different types of measurements. Measurements can be of gain, impedance, admittance and reflection. The format is magnitude (dB), real, imaginary and etc. Furthermore, it provides the maximum and minimum magnitude of the plot space.

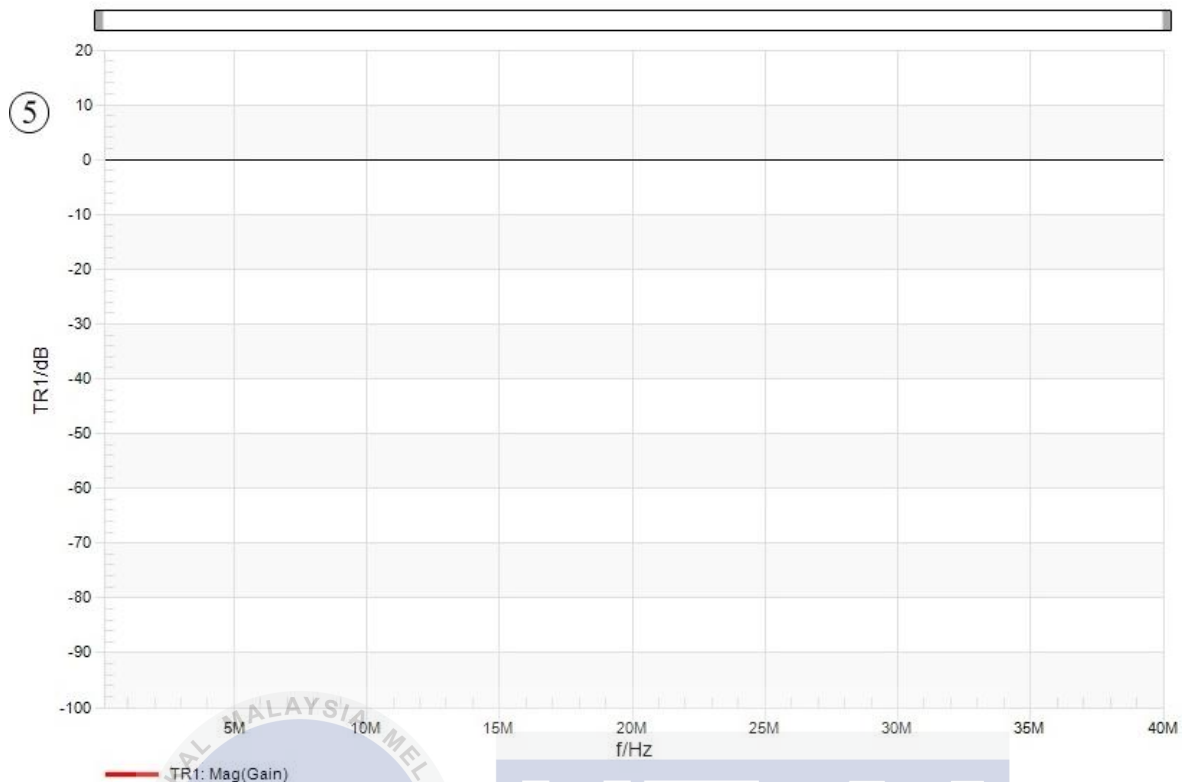


Figure 3.7: Plot Space for Graph Visualization

Figure 3.7 shows the space plot where the graph or response appeared. The X axis is always in the state of the frequency and the Y axis; depend on the desired measurements taken. The graph can be optimized to see the clear view of how the frequency response.

The connection procedure of the Bode 100 to DUT is also been studied for the validity of the data collected so the result is undeniable and correct. The connection refers to the example studied by Bode solar cell 100. Difference type of solar cells and different value of injected direct current to the solar cell is studied and to be analyzed.

3.4 Design and Development of Experimental Setup

Figure 3.8 to 3.11 below illustrate the type of DUT for this experiment and the Battery use for the injected DC voltage supplied. Figure 3.8 is a 5.5 V 0.85 W p-Si solar cell and Figure 3.9 shows 5 V 0.5 W mono-Si solar cell. For the DC voltage applied, 12 V GP battery is used (Figure 3.10) and 4 GP batteries, 1.5 V per cell is series to total up to 6 V.

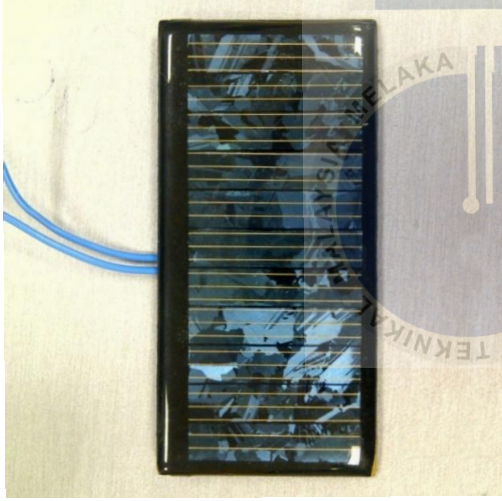


Figure 3.8: p-Si Solar Cell

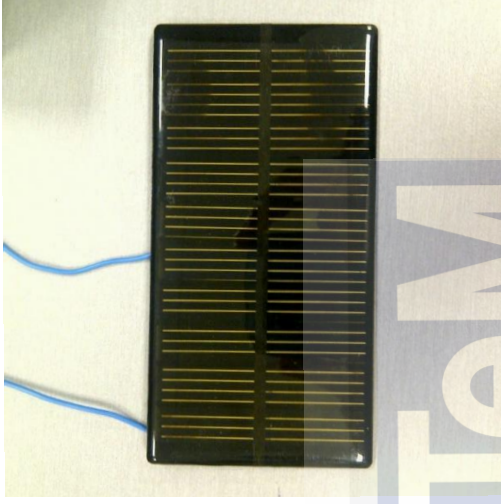


Figure 3.9: mono-Si Solar Cell



Figure 3.10: 12 V GP Battery



Figure 3.11: 4 x 1.5 V GP Battery

The purpose of setting up this experimental procedure is to obtain the wideband equivalent circuit of PV modules. Below are the simple circuit that will be derived and the parameter that will be determined.

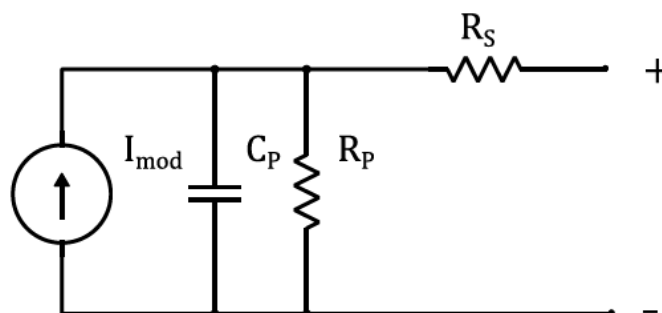


Figure 3.12: Dynamic Equivalent Circuit of PV Cell

The corresponding circuit consists of the following parameters which can resolve by the measurements detailed in this research:

- i. Parallel capacitance, C_p (consists of the diffusion - and the transition capacitance)
- ii. Parallel resistance, R_p (dynamic resistance of the diode)
- iii. Series resistance, R_s

The parallel capacitance, C_p is admittance in the circuit. Basically, admittance can be inductor or capacitor or both, but in this case it depends on the real and imaginary response of particular DUT tested. The response produced is measured in decibel (dB) unit. Not to mention, the measurement also will emphasize the response of the gain for R, L and C elements. The response of the particular graph will be used in the analysis part in which comparison technique will be executed with the response of different type of solar and DC voltage applied. The simple circuit is then can be derived using a software, Orcad Capture 9.2.

3.5 Setup Experiment Test and Data Caption

The Bode 100 is the Analyzer to be used to extract the related parameter for an equivalent circuit model of the PV cell. The impedance of a PV cell relies upon two factors; the frequency and the operating voltage of the cell which is determined by the amount of light consumed. To establish steady operation of solar driven power systems, the experiment is conducted under no-light conditions to get the impedance. Prior to the condition, the operating point is regulated by implementing a DC voltage to the cell. DC voltage will be applied to the PV cell to alter the operating point. Thus, an external device is needed to obtain that ambition. Picotest J2130A DC-Bias Injector is chosen in conjunction with the Analyzer, Bode 100.

3.5.1 High Impedance Bridge

Building the high impedance Measurement Bridge is essential for the measurement of the impedance of the PV cell. This is because the impedance of the cell is in the range of several 100 k Ω which is very high. To have a better the measurement accuracy in this impedance range, the following impedance measurement bridge is used to connect the Bode 100 to the DC Bias Injector.

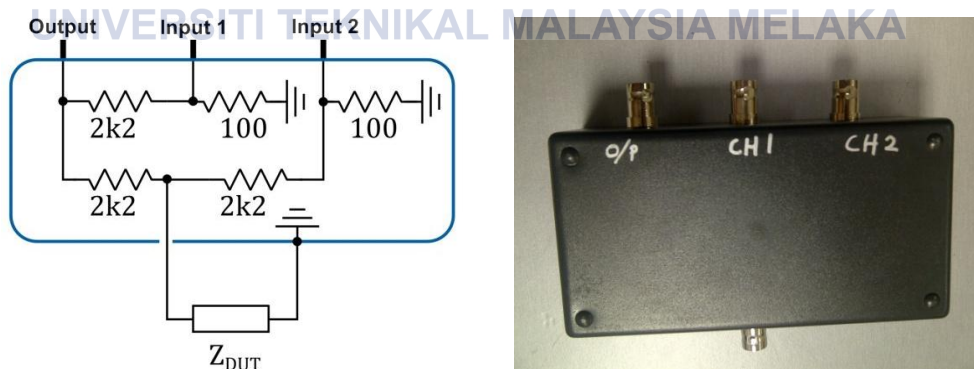


Figure 3.13: High Impedance Measurement Bridge

3.5.2 DC Bias Injector

The DC Bias Injector is used in calculating the impedance of electronic parts or devices. This is because it usually banks on many external parameters. One of the parameters is the DC Bias or DC offset. The Bode 100 often measures impedances applying an AC signal with no DC offset. In the context of solar cell measurement, the cell is biased with a DC voltage during process to ensure the Bode 100 is protected. Thus, DC Bias Injector model J2130A from Picotest is used. Figure 3.14 shows the Picotest J2130A DC Bias Injector with the DC bias voltage that is injected using a battery of 6 V and 12 V.

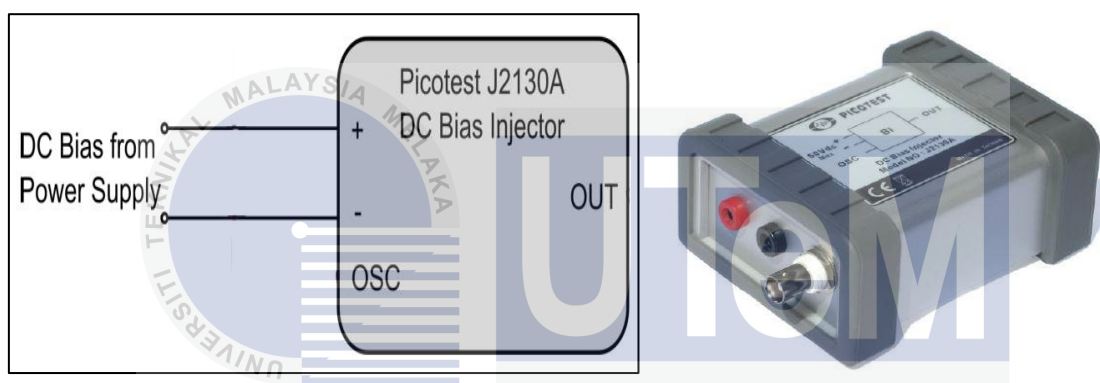


Figure 3.14: Picotest J2130A DC Bias Injector

UNIVERSITI TEKNIKAL MALAYSIA MELAKA

3.5.3 Apparatus and Tools Used in Experiment

Figure 3.15 illustrated the tool and apparatus used for this experiment. All these components function as follows:

- Laptop / PC
 - For software of Bode Analyzer Suite to run and for device configuration before the measurement is performed.
 - Data capturing device
- Bode 100
 - Measurement instrument that act as network analyser
 - Connect to High Impedance Bridge

- BNC 50 Ω coaxial cable
 - Connection medium between Bode 100 and High Impedance Bridge
 - Travel path for generated and received frequency
- BNC through male-male adapter
 - Connect the High Impedance Bridge to the DC Bias Injector.
- USB2.0 communication cable
 - Connect Bode 100 to laptop/PC for sending and retrieving information
- SMA rigid 50 Ω coaxial cable
 - Custom-made cable purposely made for connecting the DC Bias Injector to the DUT



Figure 3.15: Apparatus and Tools Used For Measurement and Data Collection Process

3.5.4 Design Set-Up of the Experiment

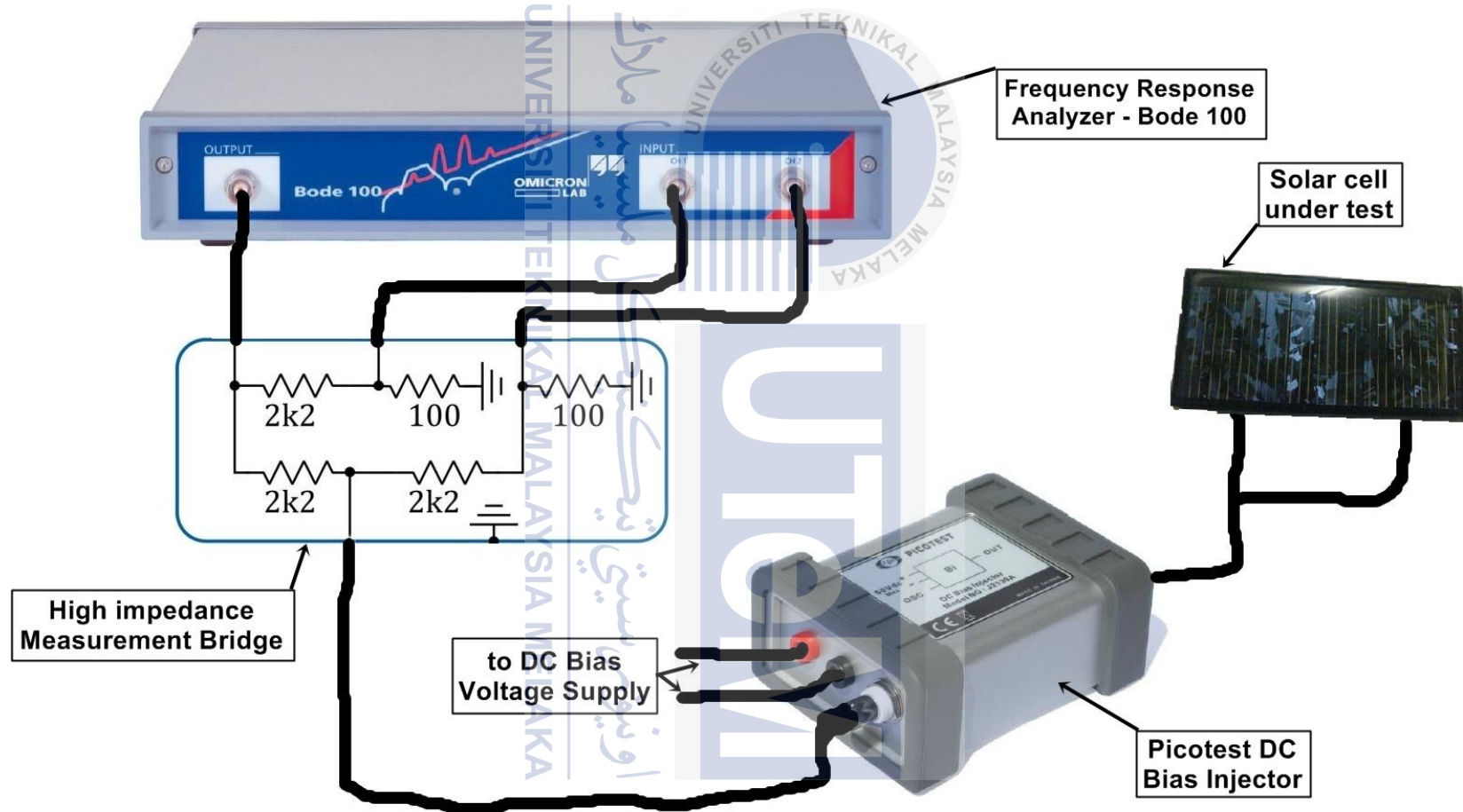


Figure 3.16: Experimental Set-Up of Bode 100 and to Solar Cell (DUT)

3.6 Device Configuration, Calibration and Obtaining the Results

After the setup is completed, Bode 100 is connected to the laptop. The software, Bode Analyzer Suite is open and configures the device. Since the experiment is measuring using High Impedance Bridge, Frequency Sweep (External Coupler) mode is chosen in the measurement mode panel. Settings of the start and stop frequency is chosen as well as the receiver bandwidth. The setting of the trace, Real and Imaginary is chosen as in Figure 3.17.

Before the measurement is taken, the device needs calibration to ensure accurate result. Three calibrations need to be performed; OPEN, SHORT and LOAD. OPEN is for the measurement of infinite impedance, it can be conducted by disconnecting the DUT to the DC bias injector output. Then, SHORT is a measurement of zero impedance, where the output is short circuited. Lastly, LOAD calibration is a certain resistance connected to the output, in this experiment $1k\Omega$ is chosen. The Interface of the calibration is illustrated in Figure 3.18. Measurement can be started.

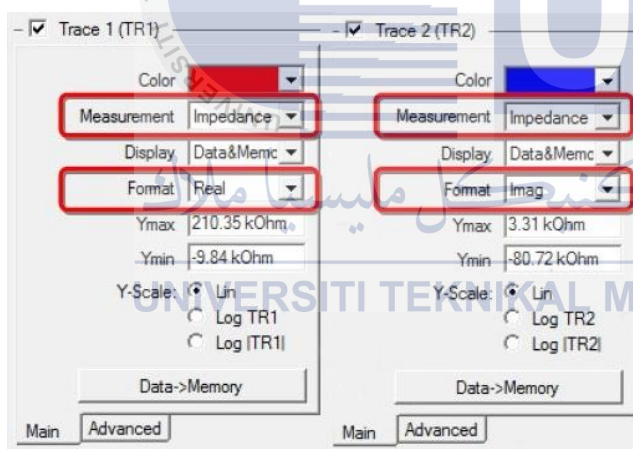


Figure 3.17: Trace 1 and Trace 2 Settings



Figure 3.18: User Calibration Interface

3.7 Data Analysis

The DUT is measured right after the single measurement setting is clicked and shows a curve of the real and imaginary trace as well as the admittance on the Cartesian grid. Now, the data analysis can be done and it involves the comparison of the particular types of the solar cell and the comparison of different DC voltage supplied. For equivalent circuit, the data can be calculated as well as measured by the Bode 100. The equation 3.1 until 3.4 is used to calculate the parameter for analysis.

$$\underline{Y} = \text{Real}(\underline{Y}) + j\text{Imag}(\underline{Y}) = \frac{1}{R_p} + j\frac{-1}{X_p} \quad (3.1)$$

Where,

$$R_p = \frac{1}{\text{Real}(Y)} \quad (3.2)$$

If $\text{Imag}(Y) < 0$:

$$C_p = \frac{1}{\omega |\text{Imag}(Y)|} \quad (3.3)$$

If $\text{Imag}(Y) > 0$:

$$L_p = \frac{|\text{Imag}(Y)|}{\omega} \quad (3.4)$$

Where,

R_p = parallel resistance

X_p = parallel reactance

C_p = parallel capacitance

L_p = parallel inductance

To enhance the comparability of the data, Microsoft Office Excel Spreadsheet is used. Nonetheless, after the parameter of the circuit is obtained the circuit is sketched in Orcad Capture 9.2.

3.8 Summary of Methodology

In this chapter, it is briefly include every detail of the process of the project as been stated in Figure 3.1 which shows the flow chart of the methodology. It is first started with the study of literature review, detailed study of FRA and design and development of experimental setup. The preparation of the material as DUT and also setup experiment test and data caption is prepared. Furthermore, the device configuration, calibration of the FRA setup and also a further data analysis is done to validate the result obtain from the measurement of FRA.



CHAPTER 4

RESULTS AND DISCUSSIONS

4.1 Introduction

In this chapter, it stated all the result obtained. There are a total of 4 responses – response of mono-Si and p-Si using 6 V and 12 V DC bias applied. Each response consists of real and imaginary curve and admittance measured. The graph is presented and visualized in a best possible way. Besides comparing the graph of the responses, parameter of the circuit is tabulated to see the clear differences between each particular response.

4.2 Description of FRA Measurements Result

In this section, all the responses in bode graph form illustrated in Figure 4.1 to 4.4 and the admittance are illustrated in Cartesian grid, shows in Figure 4.5 to 4.8. The responses are presented in the two diagrams, real and imaginary plotted for single response for observation and comparison purposes. The responses are obtained from the measurement as mentioned in Chapter 3. The responses are ranging from 10 Hz to 100 kHz injected frequency and the amplitude representing the impedance measurement itself in Ohm (Ω) unit.

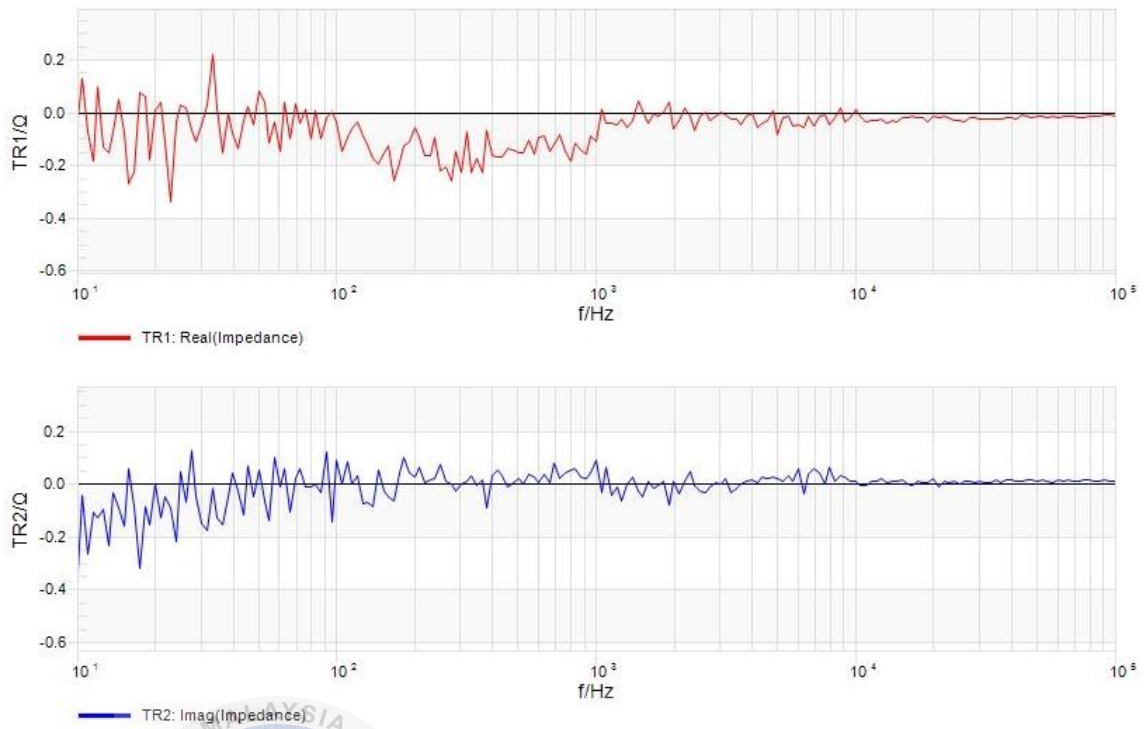


Figure 4.1: Real and Imaginary Responses of mono-Si, 6 V DC Bias Applied

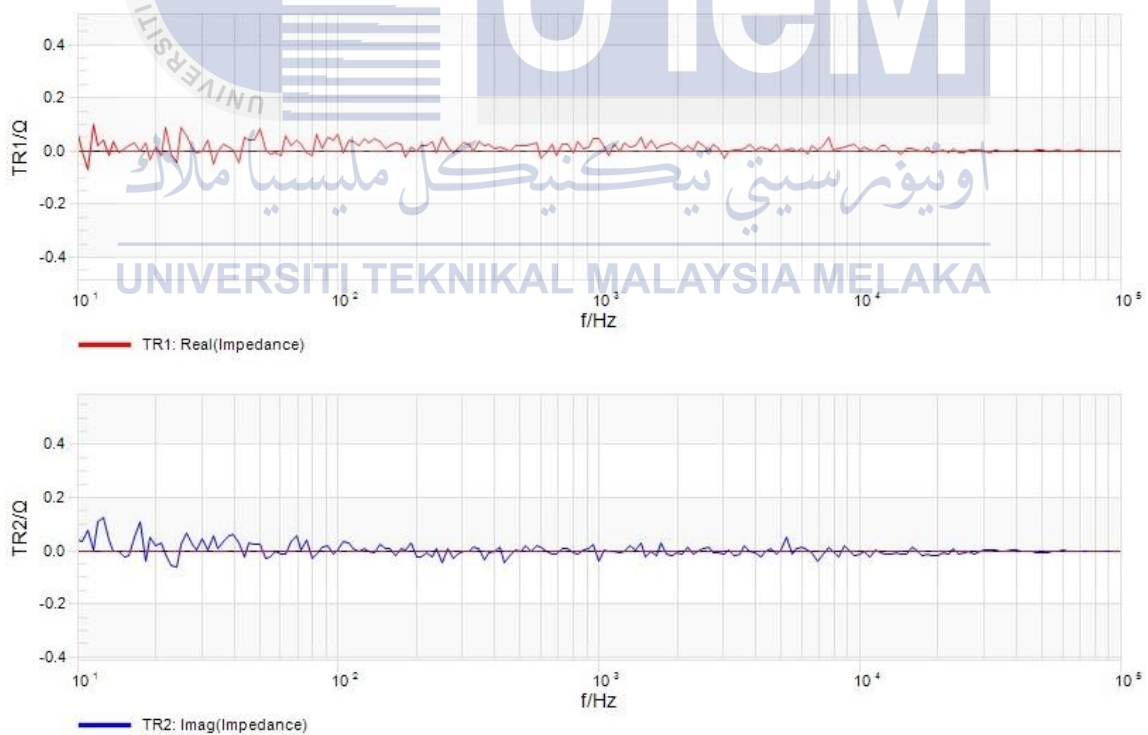


Figure 4.2: Real and Imaginary Responses of mono-Si, 12 V DC Bias Applied

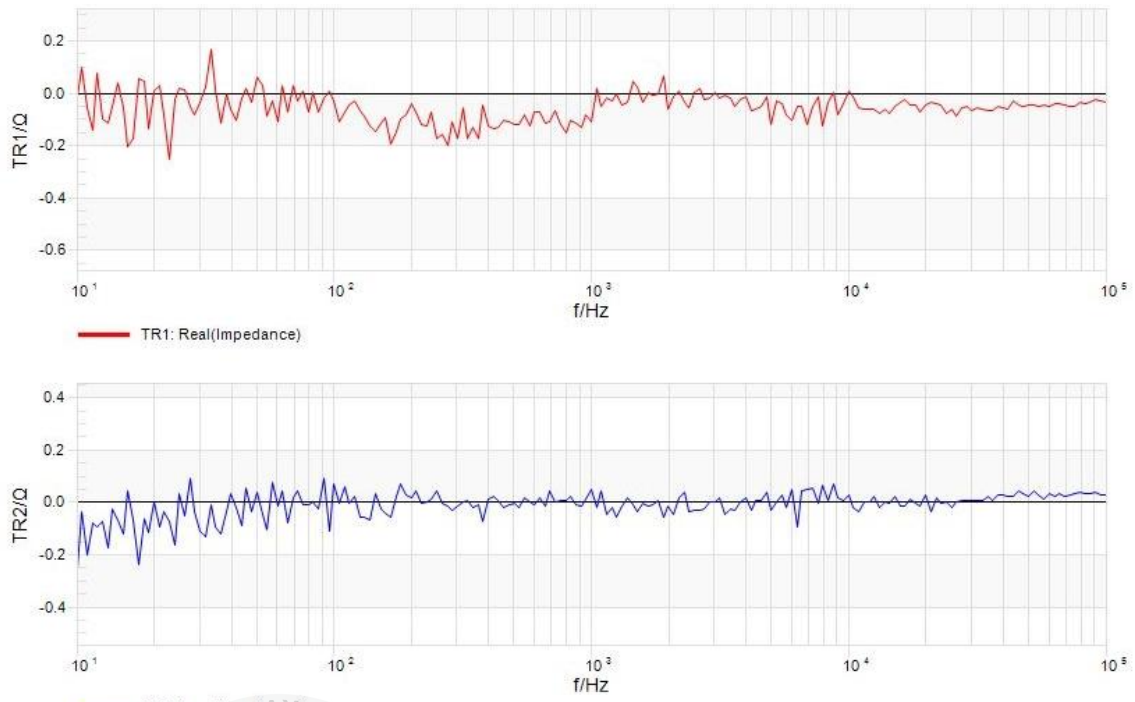


Figure 4.3: Real and Imaginary Responses of p-Si, 6 V DC Bias Applied

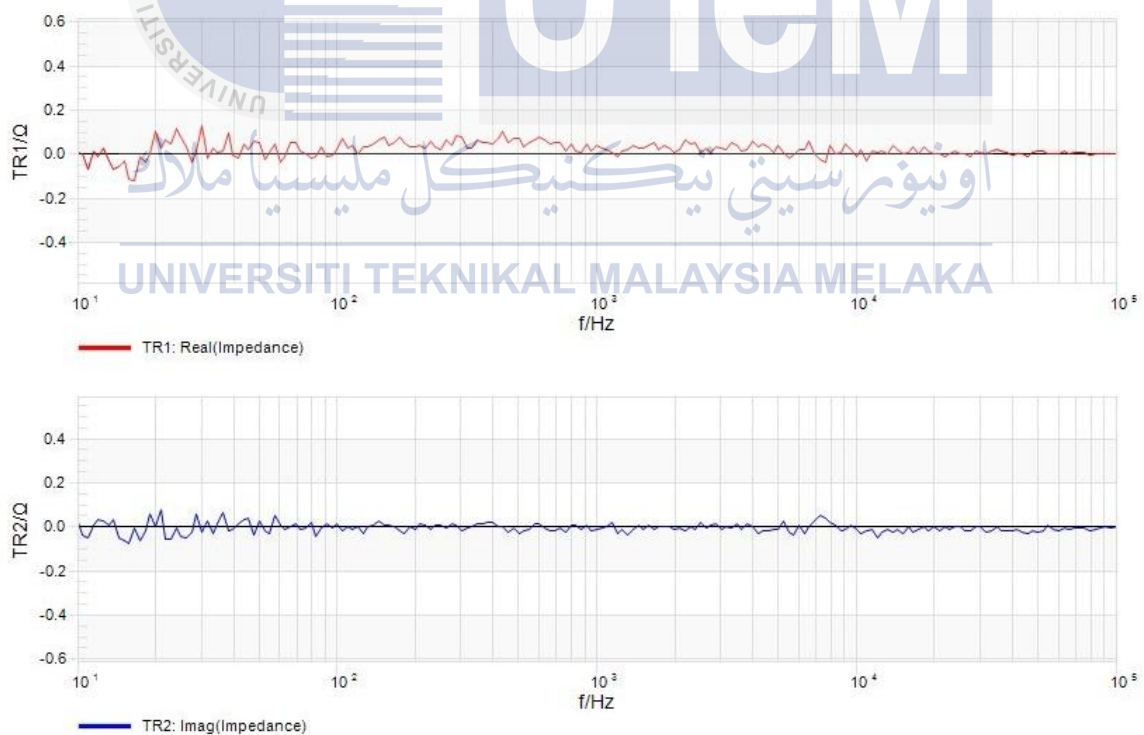


Figure 4.4: Real and Imaginary Responses of p-Si, 12 V DC Bias Applied

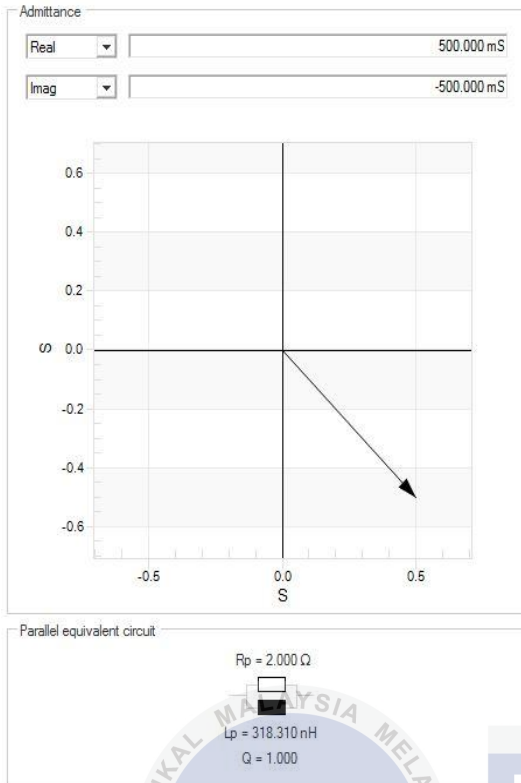


Figure 4.5: Admittance of mono-Si, 6 V DC Bias

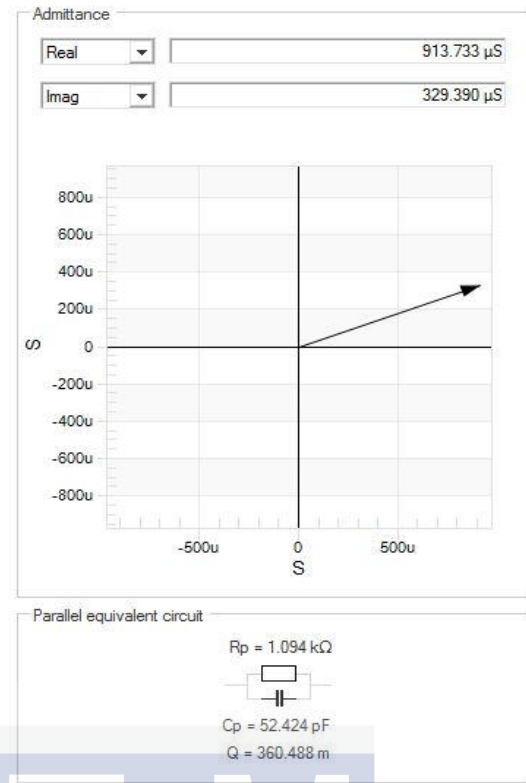


Figure 4.6: Admittance of mono-Si, 12 V DC Bias

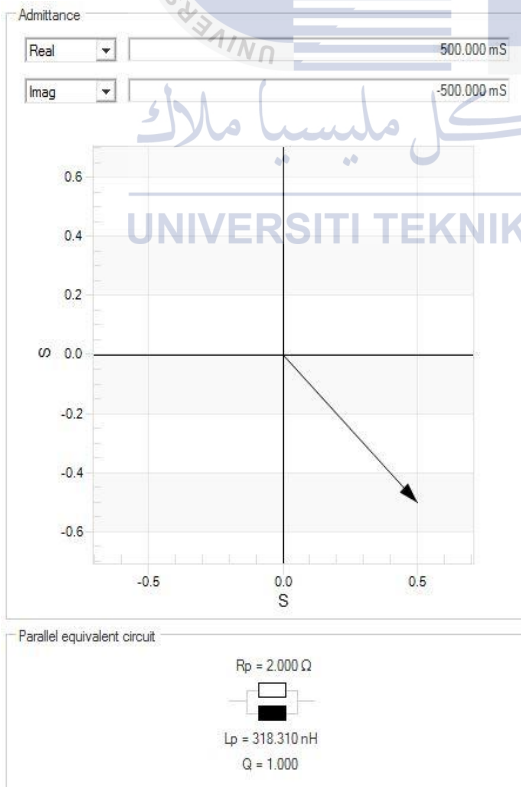


Figure 4.7: Admittance of p-Si, 6 V DC Bias

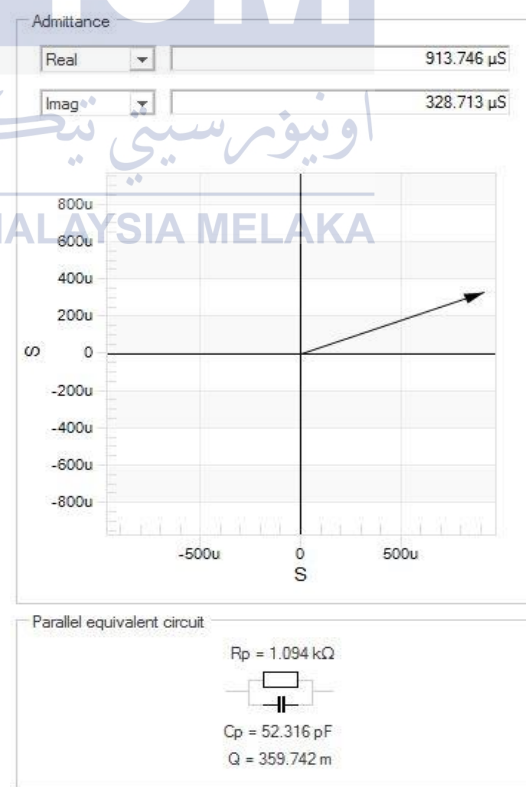


Figure 4.8: Admittance of p-Si, 12 V DC Bias

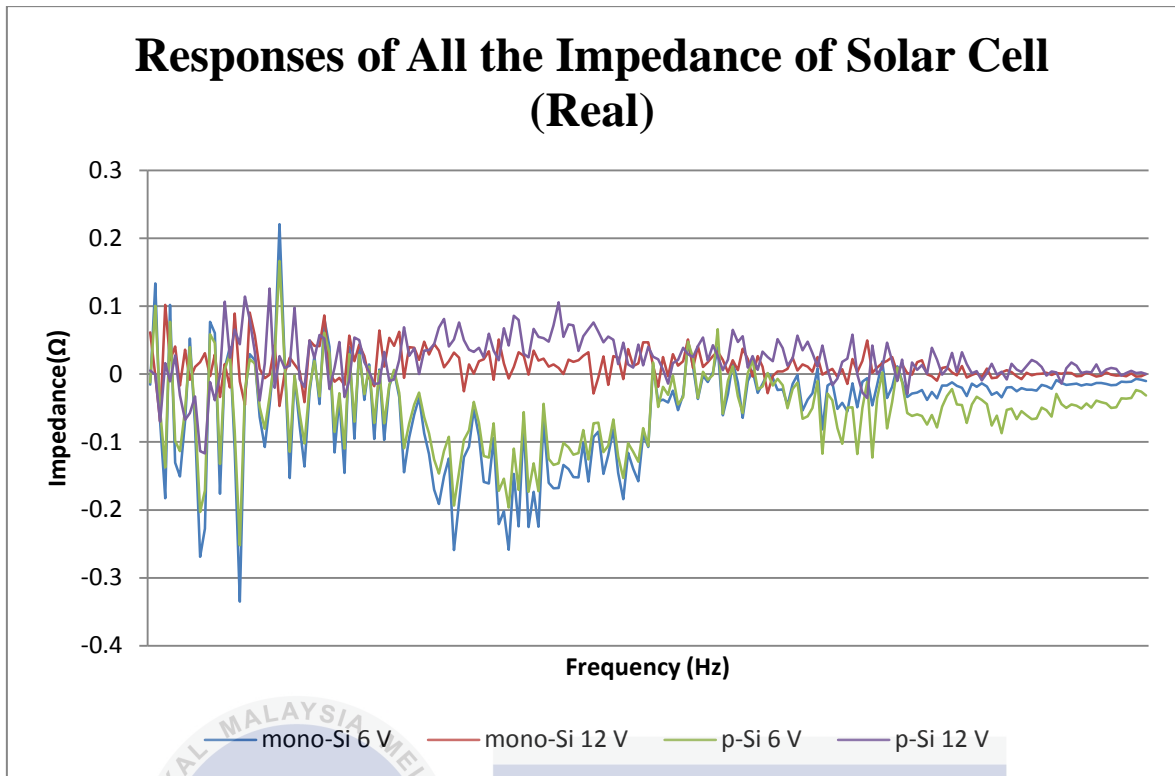


Figure 4.9: All the Real Responses of the Impedance Obtained from Experimental Procedure

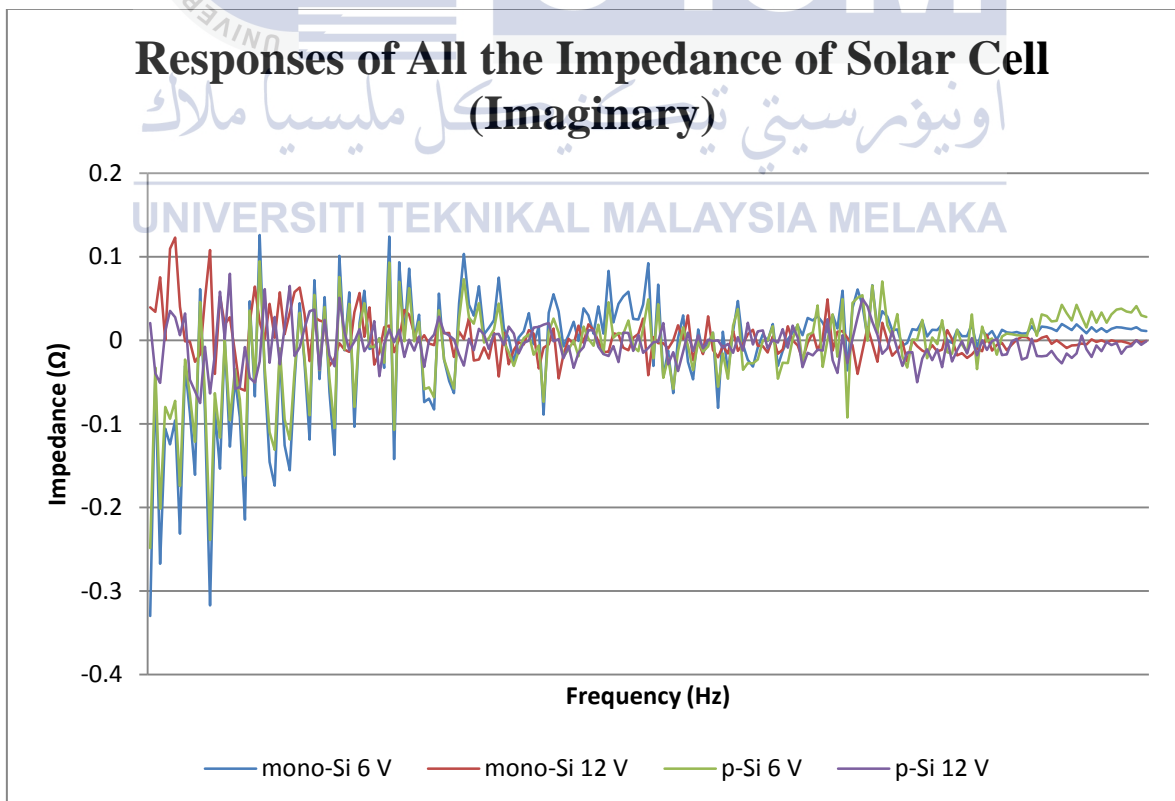


Figure 4.10: All the Imaginary Responses of the Impedance Obtained from Experimental Procedure

4.3 Observation of the Obtained Responses

As represented in Figure 4.1, 4.2, 4.3, and 4.4, observation has been made and there are similarities and differences between the responses. All the responses show much noise causing the irregular shape of the responses. The responses also show an identical form of signals, especially with the same DC voltage injected, 6 V of mono-Si (Figure 4.1) and p-Si (Figure 4.3) and 12 V of mono-Si (Figure 4.2) and p-Si (Figure 4.4). From the start of the lower frequency of 10 Hz, all the responses have an unstable attenuation. The responses continue to attenuate until 100 kHz.

In Figure 4.1, mono-Si solar cell with 6 V DC bias injected, the responses for the real part is from the range of 0.2Ω to -0.3Ω and the imaginary part is from the range of 0.2Ω to -0.3Ω . The impedance at the lower frequency is $-15.488 \text{ m}\Omega$ and at the higher frequency is $-10.395 \text{ m}\Omega$. Using the same DC Bias, p-Si solar cell has a response as shown in Figure 4.3. The response to the real part is from the range of 0.2Ω to -0.25Ω and the imaginary part is from the range of below 0.1Ω to -0.25Ω . The impedance at the lower frequency is $-12.118 \text{ m}\Omega$ and at the higher frequency is $-31.611 \text{ m}\Omega$. Both of these solar cells produce the same admittance as illustrated in Figure 4.5 and Figure 4.7. Therefore produced the identical R_p and L_p of 2.000Ω and 318.310 nH respectively.

With 12 V DC bias injected, mono-Si solar cell responses (Figure 4.2) from the range of 0.1Ω to -0.1Ω for the real part and from the range of 0.15Ω to -0.1Ω for the imaginary part. Also, the impedance at the lower frequency is $61.507 \text{ m}\Omega$ and at the higher frequency is $272.579 \mu\Omega$. Consequently, the response produces the admittance as in Figure 4.6 and derived the R_p and C_p of $1.094 \text{ k}\Omega$ and 52.316 pF . In the same way, p-Si solar cell produces almost the same outcome with the range of impedance from below 0.25Ω to -0.25Ω for the real part and below 0.1Ω to -0.05Ω for the imaginary part. At lower frequency, the response produces $5.329 \text{ m}\Omega$, higher than the value of the highest frequency which is $269.824 \mu\Omega$. Accordingly, the admittance obtained gave the R_p and C_p of $1.094 \text{ k}\Omega$ and 52.424 pF .

By using the equation at (3.1) until (3.4), the data also can be calculated manually to get the R_p and C_p or L_p . Below is a tabulation of the data obtained, for a clear observation of the difference value between the DUT. Table 4.1 illustrated the impedance

of the DUT at the lowest and the highest frequency. It clearly shows the impedances at the lowest frequency have the higher impedance compared to higher frequency, except for mono-Si solar cell with 6 V DC bias. Theoretically, the impedance at lowest frequency will always have a higher impedance. This is shown in an experiment conducted in [14] and as illustrated in Figure 2.10.

Table 4.1: Impedance of the DUT at Lowest and Highest Frequency

Solar Cell	DC Voltage (V)	Impedance (Ω) at	
		10Hz	100kHz
mono-Si	6	-15.488 m	-10.395 m
	12	61.507 m	272.579 μ
p-Si	6	-12.118 m	-31.611 m
	12	5.329 m	269.824 μ

The impedance at the highest frequency is the R_s of the circuit. The parallel resistor and parallel capacitance or inductance is derived from the measured admittance of the PV cell. Table 4.2 shows all the extracted parameters of the DUT tested.

Table 4.2: Extracted Parameters of the DUT Tested

Solar Cell	DC Voltage (V)	R_s (Ω)	R_p (Ω)	C_p (F)	L_p (H)
mono-Si	6	10.395m	2.000		318.310n
	12	272.579 μ	1.094k		52.424p
p-Si	6	31.611m	2.000		318.310n
	12	269.824 μ	1.094k		52.316p

Therefore, the following equivalent circuit model of the measured solar cell is constructed as shown in Figure 4.11 and 4.12.

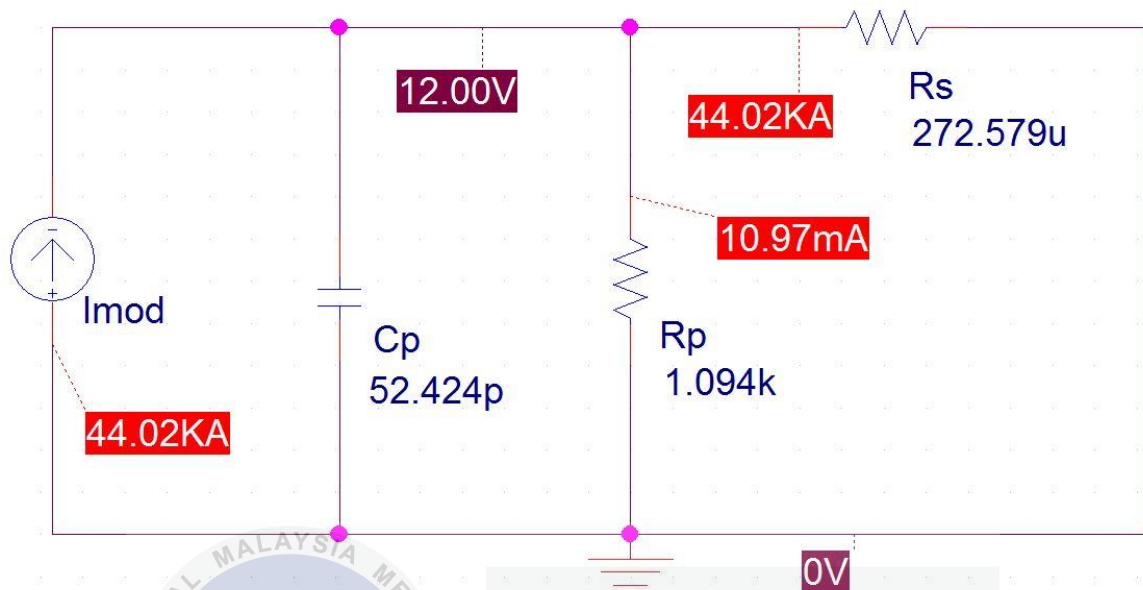


Figure 4.11: Equivalent Circuit of mono-Si Solar Cell with 12 V DC V Applied

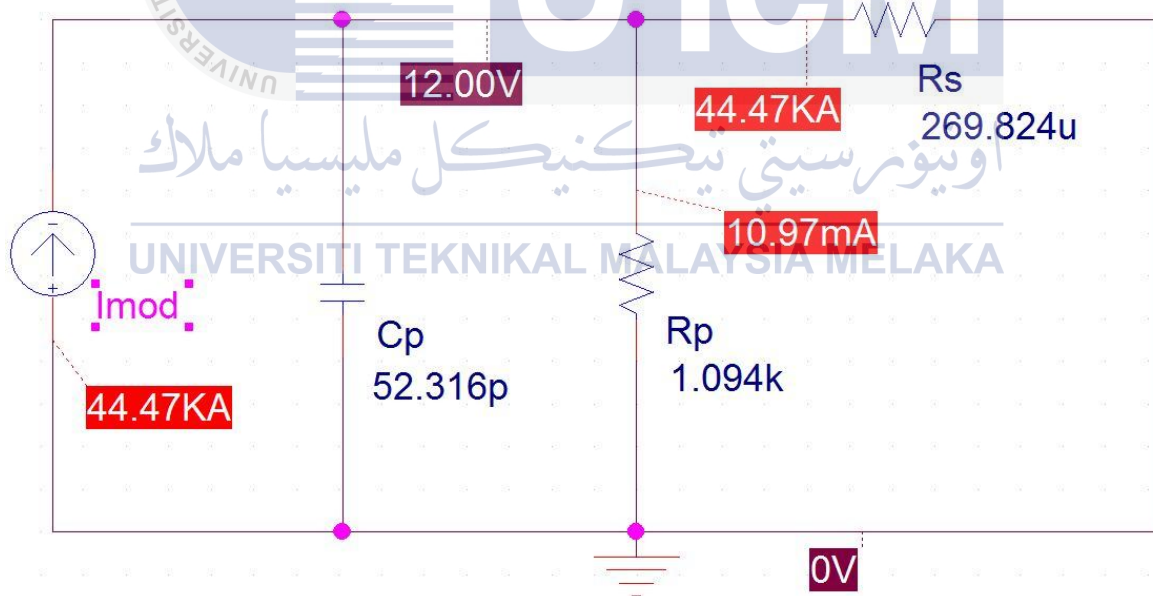


Figure 4.12: Equivalent Circuit of p-Si Solar Cell with 12 V DC V Applied

The equivalent 6 V DC bias injected circuits are shown in the Appendix A. Below is the table of the comparison between the simulated value and calculated value of 12 V DC bias applied to the both PV cells. Although, the 6 V DC bias circuits are not tabulated since its parameter is different theoretically from the expected result.

Table 4.3: Simulation and Calculation of Current for 12 V DC Bias Applied

Solar Cell	Frequency (MHz)	Impedance, Z			Current (kA)		Relative Error
		R_s ($\mu\Omega$)	R_p (k Ω)	C_p (pF)	Simulation Value	Calculation Value	
mono-Si	10	272.579	1.094	52.424	44.020	36.310	0.212
p-Si	10	269.824	1.094	52.316	44.470	36.385	0.222

The equivalent circuit of the respected tests show the simulation current value of both PV cells is much higher than the calculated value. For mono-Si solar cell, the relative error is 0.212. While, the p-Si solar cell relative error is 0.222.

4.4 Discussion of the Obtained Responses

All the response is divided to two graphs. The graph is to show the comparison of the solar cells based on the DC bias injected. Responses of real part of mono-Si vs. p-Si on 6 V DC bias (Figure 4.13) and Real part of mono-Si vs. p-Si on 12 V DC bias (Figure 4.14) is illustrated below along with further discussion.

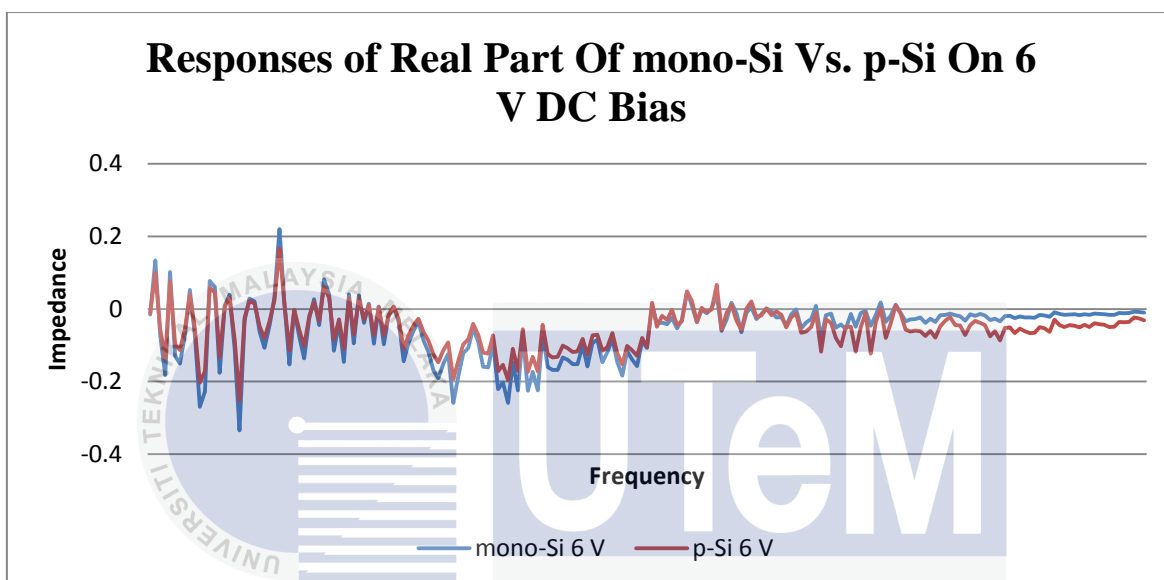


Figure 4.13: Responses of Real Part of Mono-Si vs. Poly-Si on 6 V DC Bias

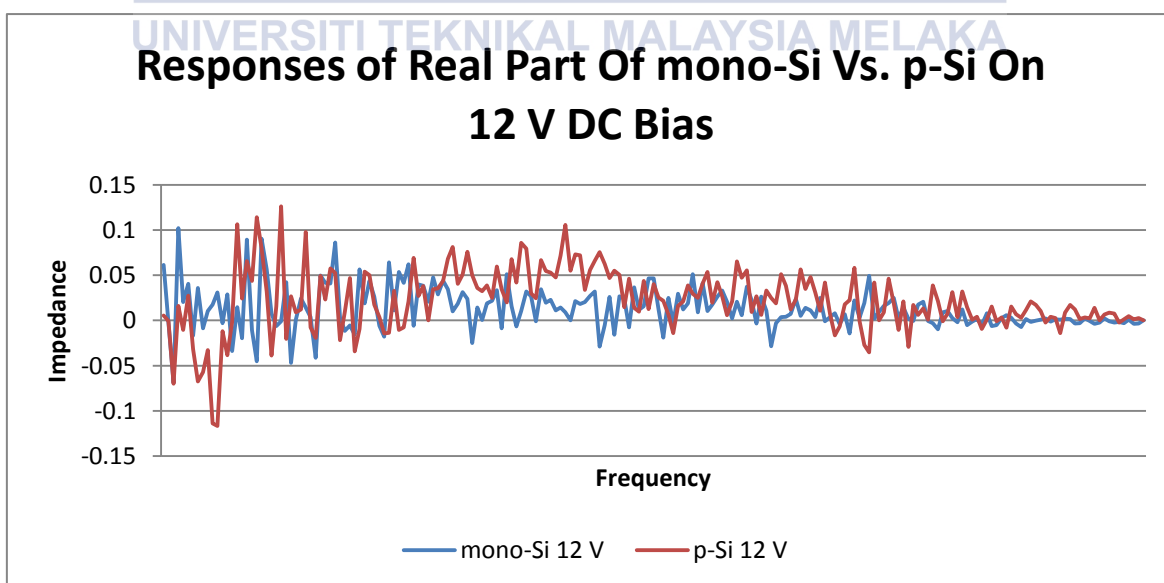


Figure 4.14: Responses of Real Part of Mono-Si vs. Poly-Si on 12 V DC Bias

Both graphs show a huge difference, especially on the result of the parameter extracted. Figure 4.13 especially, the result is inaccurate, according to the theoretical explanation in Chapter 2 of Figure 2.10 and Figure 2.11. Under that circumstance, the results produce the capacitance value of the parallel admittance along with the resistor. Instead, the responses show an inductive value. On the contrary, responses in Figure 4.14 produce a theoretically correct result, which derived a parallel capacitor along with series and parallel resistor. The use of high DC bias voltage is a main factor that affects the responses, giving only slight differences between the lower frequency and higher frequency. Referring to work in [14] on Figure 2.11, the lower the voltage per cell injected into the solar cell, the higher the impedance at lower frequency. However, at the lower frequency, all the responses end at the same impedance which is the impedance of the series resistor, R_s .

Among the significance and implication of the findings are to create switching power conditioner that is adequate, decent, eminent power and small-scale and in order to achieve that detailed understanding of both DC and AC attribute of the PV cells especially the capacitance is essential. Not only most of the AC corresponding circuit is able clarified by dynamic characteristics of solar cells [16] but also impedance in a solar cell is a critical specification to observe as it is symbolic of the aging and consequences of sustaining life period of the solar cell. As mentioned in [17], variations in this parameter deriving out of guideline shall be applied to evaluate the aging period or fault in the solar cell. The result of the experiment can be applied to ensure the stability of solar driven power systems, especially solar cell arrays and voltage regulators.

4.5 Summary of Results and Discussion

All of the results of the responses are shown and discussed. It is declared that result of the experiment on 12 V DC bias applied shows the expected parameter though the responses shaped is different from the theoretical explanation in previous work. On the other hand, the result of the experiment on 6 V DC bias applied shows a different outcome. Totally different from the expected result, responses are inaccurate after the theoretical fact is explained. The significance and application of the findings are discussed.

CHAPTER 5

CONCLUSION

5.1 Conclusion

Implementation of solar cell as DUT using FRA is successfully done. As stated in the objectives, the function of the FRA device, Frequency Response Analyzer Bode 100 on a solar cell is well studied. An experimental test for FRA Network Analyzer Bode 100 to a solar cell also is analyzed with well presentation of the result and discussion. Then, the dynamic impedance of solar cell relationship between different types of solar cells and on different range of DC bias injected to solar cells is studied. It can be concluded that this project is successful since all the objectives are achieved. The implementation of this type of testing of solar cell is applicable as the results of this measurement can be used to derive a dynamic small signal model of the solar cell. Equivalent models of the solar cells will help to ensure the stability of solar driven power systems, especially solar cell arrays and voltage regulators.

5.2 Recommendation

For further research of impedance in solar cell using Frequency Response Analysis, it is recommended to use the appropriate DC bias applied to the solar cell. The voltage of below 1.0 V is advisable to ensure a concrete result and to minimize error in the responses. An ambience condition of the experiment is also a huge factor to the response; the solar cell must be in a dark condition to get a precise and accurate result to the extracted parameter. In addition, other different types of solar cells, such as amorphous silicon, Cadmium Telluride, Copper Indium Gallium Selenide and organic photovoltaic cells can be considered to be tested therefore within the scope of the research in the future.



REFERENCES

- [1] Ryder, S.A., Diagnosing Transformer Faults Using Frequency Response Analysis, IEEE Electrical Insulation Magazine, vol.19, pp. 16-22, 2003.
- [2] M. A., Green, *Solar Cells - Operating Principles, Technology and System Application*. 1st ed.. Kensington: Prentice-Hall, 1992.
- [3] P. E. Wellstead, Frequency response analysis, Solartron analytical, Solartron Instruments, Hampshire, England, Tech. Rep. 1999.
- [4] Silicon Materials and Devices R&D. [online], Available at: http://www.nrel.gov/pv/silicon_materials_devices.html (National Renewable Energy Laboratory) [accessed 6 November 2013]
- [5] M., Zeman, Photovoltaic Systems, Solar Cells, [online], Available at: http://ocw.tudelft.nl/fileadmin/ocw/courses/SolarCells/res00029/CH9_Photovoltaic_systems.pdf (Delft University of Technology) [accessed 26 June 2014]
- [6] D.S. Kim, A.M.Gabor, V.Yelundur, A.D. Upadhyaya, V. Meemongkolkiat A.Rohatgi, *String-Ribbon Silicon Solar Cells with 17.8 % efficiency*, Proceedings of the 3rd World Conference on Photovoltaic Energy Conversion, 2003
- [7] Types of Thin Film Solar Cells, *Making Thin Film Solar Cells*, [online]. Available at: http://www.tf.uni-kiel.de/matwis/amat/semitech_en/kap_8/backbone/r8_3_1.pdf (Faculty of Engineering at Kiel University) [accessed 26 June 2014]
- [8] D, Appleyard, Utility-Scale Thin-Film: Three New Plants in Germany Total Almost 50 MW, Available at: <http://www.renewableenergyworld.com/rea/news/article/2009/03/utility-scale-thin-film->

[three-new-plants-in-germany-total-almost-50-mw?cmpid=WNL-Friday-March13-2009](http://www.renewableenergyworld.com/news/2009/03/13/three-new-plants-in-germany-total-almost-50-mw?cmpid=WNL-Friday-March13-2009)

(Renewable Energy World Magazine) [accessed 9 November 2013]

[9] *Industry Benchmark Thin Film Modules*, [online], Available at: <http://www.firstsolar.com/Innovation/Advanced-Thin-Film-Modules> (First Solar) [accessed 8 November 2013]

[10] T. P., Hough, *Trends in Solar Energy Research*, Nova Publishers, New York.

[11] D. Chenvidhya, PV Grid-Connected Systems for Residential Distribution System: Dynamic Impedance Characterization of Solar Cells and PV modules; Doctor of Engineering Thesis. King Mongkut's University of Technology Thonburi; Bangkok, Thailand; 2002.

[12] R.A. Kumar, M.S. Suresh, J. Nagaraju. Measurement of AC parameters for Gallium Arsenide (GaAs/Ge) solar cell by impedance spectroscopy, *IEEE Trans Electron Devices*, Vol. 48, pp. 2177-2179, 2001

[13] R.L. Mueller, M.T. Wallace, and P. Illes, Scaling nominal solar cell impedances for array design, *Proc. IEEE First WCPEC*, pp. 2034-2037, 1994.

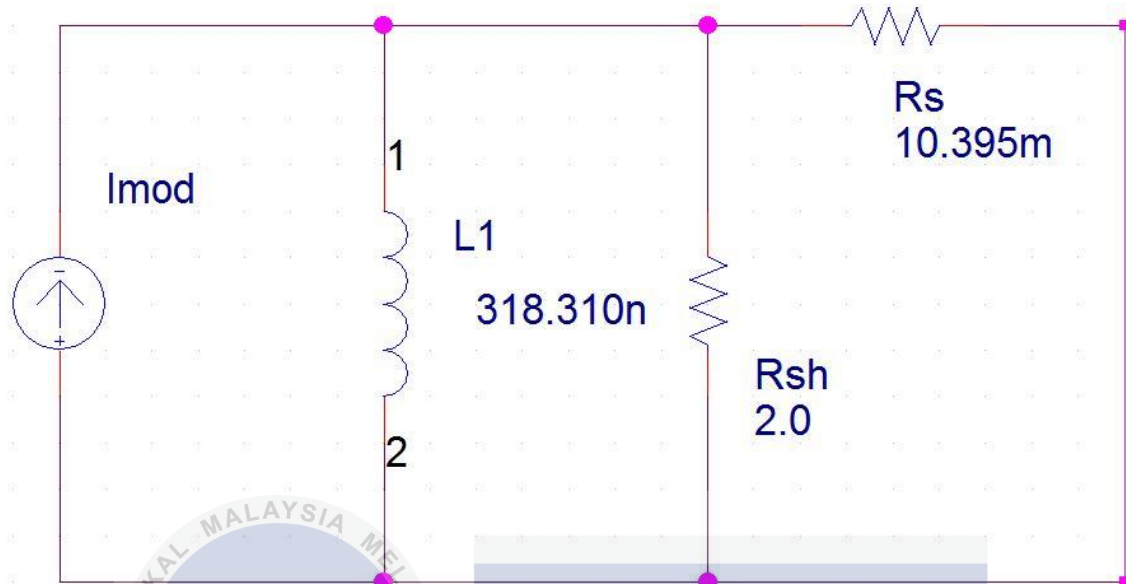
[14] Omicron Lab, Solar Cell Impedance Measurement using the Bode 100, V1.1, Omicron Electronics GmbH 2012.

[15] R. A. Kumar, Measurement of solar cell AC parameters using impedance spectroscopy, M.S. thesis, Indian Institute of Science, Bangalore, India, Jan. 2000.

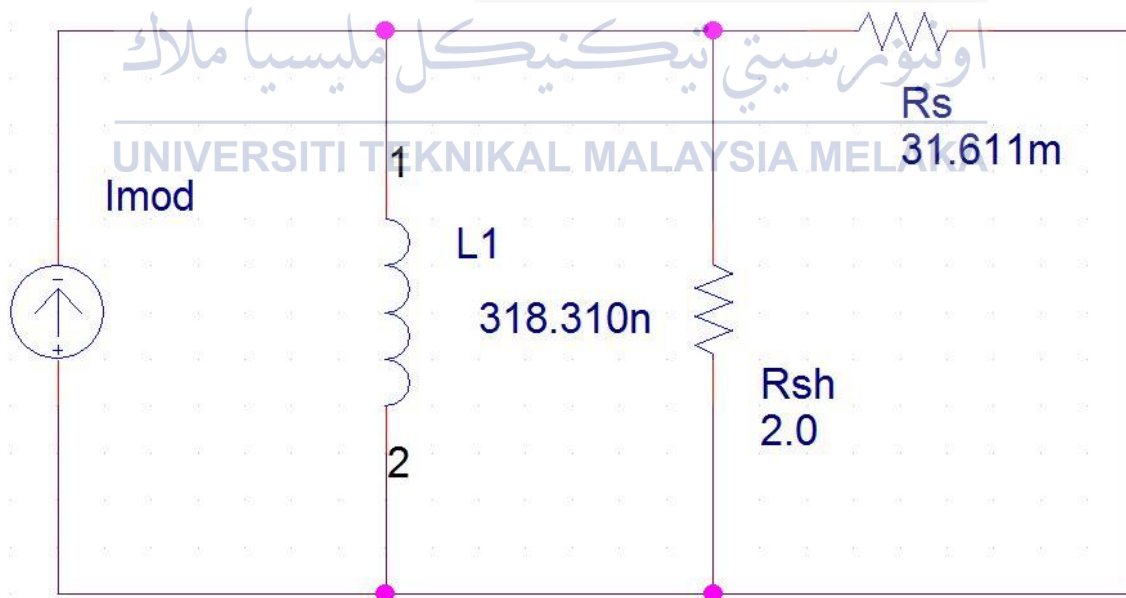
[16] R. A. Kumar, Studies on Solar Cell AC Parameters, Doctoral thesis, Indian Institute of Science, Bangalore, India, 2004.

[17] S. P. Bharadwaj, A. E. Ginart, I. N. Ali, P. W. Kalgren, J. Celaya, and S. Poll, Solar Cells Aging Estimation Based On Impedance Characterization, *IEEE Aerospace Conference 2011*, pp. 1-9, 2011.

APPENDIX A



Equivalent Circuit of Mono-Crystalline Solar Cell with 6 V DC Bias Applied



Equivalent Circuit of Poly-Crystalline Solar Cell with 6 V DC Bias Applied

APPENDIX B

PSM

ORIGINALITY REPORT

27 %	24 %	4 %	11 %
SIMILARITY INDEX	INTERNET SOURCES	PUBLICATIONS	STUDENT PAPERS

PRIMARY SOURCES

1	energyinformative.org <i>Internet Source</i>	11%
2	www.solarbc.ca <i>Internet Source</i>	7%
3	ph-jakobsen.dk <i>Internet Source</i>	3%
4	www.electrical4u.com <i>Internet Source</i>	2%
5	R.A. Kumar. "Measurement of AC parameters of gallium arsenide (GaAs/Ge) s... <i>Publication</i>	1%
6	Submitted to McMaster University <i>Student Paper</i>	1%
7	Perny, M., M. Kusko, V. Saly, and J. Packa. "PV concentrator cells complex im. <i>Publication</i>	< 1%
8	www.truevaluesolar.com.au <i>Internet Source</i>	< 1%
9	eprints.utar.edu.my <i>Internet Source</i>	< 1%
10	Mette, Ansgar. "New concepts for front side metallization of industrial silicon s... <i>Publication</i>	< 1%
11	Submitted to Gwynn Park High School <i>Student Paper</i>	< 1%
12	Submitted to Marist College <i>Student Paper</i>	< 1%
13	Zanuccoli, Mauro <1974>(Fiegna, Claudio). "Advanced Numerical Simulation ... <i>Publication</i>	< 1%
14	Reinders, A.H.M.E., and W.G.J.H.M. van Sark. "Product-Integrated Photovolt... <i>Publication</i>	< 1%
15	solarno.hr <i>Internet Source</i>	< 1%

APPENDIX B

16	uniteusforclimate.org <i>Internet Source</i>	< 1%
17	G.A. Landis. "Wide-bandgap epitaxial heterojunction windows for silicon solar..." <i>Publication</i>	< 1%

EXCLUDE QUOTES ON
EXCLUDE BIBLIOGRAPHY ON

EXCLUDE MATCHES OFF



اونيورسيتي تيكنيكل مليسيا ملاك

UNIVERSITI TEKNIKAL MALAYSIA MELAKA